universität wien

MASTERARBEIT / MASTER'S THESIS

Titel der Masterarbeit / Title of the Master's Thesis

„DNA BARCODING OF TERRESTRIAL ISOPODS IN AUSTRIA INTEGRATING MUSEUM SPECIMENS"

verfasst von / submitted by

Anna-Chiara Barta, BSc

angestrebter akademischer Grad / in partial fulfilment of the requirements for the degree of

Master of Science (MSc)

Wien, 2023 / Vienna, 2023

Studienkennzahl lt. Studienblatt / degree programme code as it appears on the student record sheet:	UA 066 831
Studienrichtung lt. Studienblatt / degree programme as it appears on the student record sheet:	Masterstudium Zoologie
Betreut von / Supervisor:	Mag. Dr. Luise Kruckenhauser
Mitbetreut von / Co-Supervisor:	Dr. Martin Schwentner

Acknowledgements

I would like to thank Martin Schwenter for introducing me to the intriguing yet often intricate field of molecular research but also for his essential contributions to the study. His constant support, patience and valuable guidance were of great importance. In addition, Martin performed the morphological work for the study and made significant contributions to the analysis of the Illumina sequence data. His dedication and expertise played a vital role in this research.

I would also like to express my deep gratitude to Luise Kruckenhauser for her mentoring, sharing her extensive knowledge and invaluable support.

My sincere thanks go to the dedicated team of the Central Research Laboratories Department and the Third Zoology Department of the Natural History Museum. Their support, feedback, and quick troubleshooting were indispensable. A special mention goes to Tricia Goulding, who contributed with her expertise and help in the lab.

I'm immensely grateful to the numerous individuals who participated in the extensive isopod collecting efforts in the field, particularly Stefan Koblmüller, Matthäus Greilhuber, and Christoph Leeb. Their collaboration significantly enriched this study.

Last, but certainly not least, I owe thanks to my family. Their contributions in collecting the Vorarlberg species and their tireless support inside and outside my working environment have been of utmost importance to me.

Abstract

Oniscidea, a diverse group of terrestrial Isopods, demonstrate remarkable global diversity. In Austria, there are 64 oniscidean species, but many are not represented in DNA barcoding databases.

Analyzing 317 sequences of the cytochrome c oxidase I (COI) region, DNA barcodes from 29 Oniscidea species were generated. The majority of species displayed a maximum intraspecific distance below 6%, with *Armadillidium vulgare* (6.5%) and *Cylisticus convexus* (6.3%) slightly exceeding this threshold. Certain species exhibited remarkably high intraspecific distances, including *Porcellium collicola* (13.9%), *Trachelipus ratzeburgii* (10.4%), and *Tracheoniscus pusillus* (11.7%), hinting at potential cryptic species. This interpretation is further supported by species delimitation analyses, including ASAP and GMYC, which divided the dataset into 34-51 putative species.

Additionally, this study tested the utility of historical isopod specimens dating from 1880 to 1968, despite challenges like limited DNA content and fragmentation. This resulted in the acquisition of 17 valuable COI barcode sequences from the historical collection of the NHM Vienna through the implementation of two different approaches. Mini-barcode amplification, involving short COI fragments via Sanger sequencing, outperformed Next-Generation Sequencing (NGS) via genome skimming in this study. Nevertheless, a protocol for Illumina Sequencing of historical specimens was established designed to address issues like formalin-fixation damage and high proportions of single-stranded DNA (ssDNA). These DNA-barcode sequences, obtained from historical museum specimens, play an important role in bridging gaps in the representation of rare species, thus supporting DNA barcoding initiatives like the Austrian Barcode of Life (ABOL).

Zusammenfassung

Oniscidea ist eine diverse Gruppe terrestrischer Isopoden und zeigt eine beeindruckende globale Vielfalt. In Österreich gibt es 64 Oniscidea-Arten, von denen jedoch viele bisher in DNA-Barcoding-Datenbanken nicht repräsentiert sind.

Durch die Analyse von 317 Sequenzen der Cytochrom c Oxidase I (COI) Region wurden DNA-Barcodes von 29 Oniscidea Arten erstellt. Die meisten Arten wiesen eine maximale intraspezifische Distanz von weniger als 6 % auf, wobei *Armadillidium vulgare* (6,5 %) und *Cylisticus convexus* (6,3 %) dies leicht übertrafen. Einige Arten wiesen bemerkenswert hohe intraspezifische Distanzen auf, darunter *Porcellium collicola* (13,9 %), *Trachelipus ratzeburgii* (10,4 %) und *Tracheoniscus pusillus* (11,7 %), was auf potentielle kryptische Arten hindeutet. Diese Interpretation wird durch Artenabgrenzungsanalysen, einschließlich ASAP und GMYC, unterstützt, die den Datensatz in 34-51 mutmaßliche Arten unterteilten.

Darüber hinaus wurde im Rahmen dieser Studie der Einsatz historischer Proben aus der Zeit von 1880 bis 1968 getestet, trotz Herausforderungen wie geringem DNA-Gehalt und Fragmentierung. Dies führte zur Generierung von 17 wertvollen COI-Barcode-Sequenzen aus der historischen Sammlung des NHM Wien durch die Anwendung zweier verschiedener Ansätze. Gegenüber dem Next-Generation Sequencing (NGS) durch Genome-Skimming führte die Amplifikation von Mini-Barcodes (kurze COI-Fragmente) mittels Sanger-Sequenzierung in dieser Studie zu mehr erzeugten Sequenzen. Nichtsdestotrotz wurde ein Protokoll für die Illumina-Sequenzierung historischer Proben entwickelt, um Probleme wie Formalin-Fixierungsschäden sowie hohe Anteile an einzelsträngiger DNA (ssDNA) zu beheben. Diese DNA-Barcode-Sequenzen, die aus historischen Museumsexemplaren gewonnen werden, spielen eine wichtige Rolle bei der Überwindung von Lücken in der Darstellung seltener Arten und unterstützen damit DNA-Barcode-Initiativen wie den Austrian Barcode of Life (ABOL).

Content

Introduction

1. Isopoda

Isopods, a diverse group of crustaceans, belong to the class Malacostraca. Their habitat spans a remarkable spectrum, ranging from deep-sea to an array of terrestrial environments, including mountains and caves. Their species count worldwide stands at around 10,668 including marine species (Boyko et al., 2008). Over time, numerous synonyms and subspecies have been proposed, reflecting both the diversity and the challenges in taxonomy and species delineation within this group (Schmalfuss 2003).

The suborder Oniscidea, encompassing terrestrial isopods or woodlice, is a subject of ongoing debate regarding its monophyletic nature (Dimitriour et al. 2019, Tabacaru & Giurginca 2021). Oniscidea have been historically recognized for its many morphological synapomorphies (Schmalfuss 2003, Schmidt 2008). What characterizes these species is their remarkable adaptability to diverse terrestrial environments, particularly those with moisture, although some can thrive in arid regions (Schmidt 2008). Unlike other terrestrial crustaceans, they do not depend on open water for their reproduction because their early development unfolds within a marsupium, a protective brood pouch on the ventral side of the female (Schmidt 2008). Notably, certain species, including *Ligia* and *Olibrinus*, have even adapted to an amphibious lifestyle along seashores, while a rare few, such as *Haloniscus*, have conquered hypersaline conditions, and others, like *Typhlotricholigioides*, have ventured into subterranean waters (Schmidt 2008). These astonishing adaptations underscore the versatility of Oniscidea in responding to diverse ecological conditions. Austria hosts 64 recognized species of Oniscidea, with earlier listings including an additional 14 subspecies that have been synonymized over time (Schmalfuss 2003; Strouhal 1951). These Austrian Oniscidea species can be categorized into four lineages: Crinocheta, Ligiidae, Mesoniscidae, and Synocheta. The Crinocheta lineage comprises Agnaridae (five species),

Armadillidiidae (nine species), Cylisticidae (one species), Oniscidae (two species), Philosciidae (four species), Platyarthridae (one species), Porcellionides (four species), and Trachelipodidae (ten species). Ligiidae only includes only two species, Mesoniscidae one, and Synocheta exclusively encompassess Trichoniscidae, totaling 25 species.

2. DNA Barcoding of Austrian Isopods

DNA barcoding is a molecular genetic technique that offers a convenient alternative to morphology-based identifications, addressing challenges such as the classification of juveniles, species with strong sexual dimorphism, or damaged specimens (Kress & Erickson 2012). This is especially relevant for Oniscidea, as species-level morphological identifications often hinge on male-specific characteristics of the pleopods and/or the 7th thoracopods. DNA barcoding involves a short gene sequence of a standardized part of the genome, namely a DNA barcode, as an identifier for different taxa. For most animal phyla a fragment of the cytochrome c oxidase I gene (COI) is used. The DNA barcode sequence of the unknown specimen is then compared with a digital DNA barcode database (eg. BOLD Barcode of Life Database; Hebert et al. 2003). Universality is a key advantage, as COI can be applied across diverse organisms, aiding taxonomists in identifying cryptic or novel species and facilitating cross-species comparisons (Hebert et al. 2004). This is achieved through the comparison of both intra- and interspecific genetic divergences. Austria contributes to this effort through the Austrian Barcode of Life (ABOL) project, aimed at building a reference library of DNA barcodes for all Austrian animals, plants and fungi. However, challenges arise as this method relies on comprehensive reference databases, with the Barcode of Life Data Systems (BOLD) serving as a central repository for DNA barcoding data. A considerable part of the 64 oniscidean species and subspecies of Austria has not yet received an entry in the database, highlighting the need for a DNA barcoding database for Austrian species.

In 2022, Raupach et al. established the first comprehensive DNA barcode library for German isopods, encompassing 46 of the 57 terrestrial and freshwater species present in Germany. Notably, Germany hosts a smaller number of isopod species compared to Austria, and there are also unique species in Germany that do not occur in Austria. Their research findings unveiled remarkably high levels of intraspecific genetic variation within the COI region for numerous species. Even seemingly well-known and common species, such as *Porcellio scaber*, exhibit strikingly high intraspecific genetic distances, with a maximum observed distance of 12.16%. Similarly, *Trachelipus rathkii* shows considerable intraspecific genetic variation, reaching a maximum distance of 16.59%. These results align with several other studies on both marine and terrestrial isopod species, which have also reported substantial genetic diversity, some, suggesting the presence of cryptic species (Bedek et al. 2019, Bober et al. 2019, Brix et al. 2014, Delhoumi et al. 2019, Eberl et al. 2013, Klossa-Kilia et al. 2005, Parmakelis 2008, Paulus et al. 2022). This raises the intriguing possibility of similar cryptic diversity within Austrian isopod species.

In the context of extensive discussions regarding DNA barcoding, it's vital to stress that while DNA can be a useful tool for confirming known species and providing insights into potential new ones, it should not serve as the sole method for comprehensive species discovery, rigorous hypothesis testing, constructing intricate phylogenetic trees, or establishing formal classifications (Bober et al. 2019, Brower et al. 2010, Meier et al. 2006, Tan et al. 2010, Will et al. 2005). Challenges stem from the intricate genetic variations among populations, which can result in either wrongly grouping recently diverged species or splitting long-established ones (Meier et al. 2006, Meyer & Paulay 2005, Tan et al. 2010). The application of fixed thresholds for species identification is not always effective, given the considerable overlap between differences within and between species (Meier et al. 2006, Meyer & Paulay 2005).

3. Natural History Collections and DNA Barcoding

The Natural History Museum of Vienna harbors a substantial isopod collection, comprising 5383 lots from Austria. Within this collection, around 120 different species and subspecies are represented, although it's important to note that some of these taxonomic designations may not be currently accepted and could require revision. Notably, these specimens were determined by the isopod expert, Hans Strouhal (* October 2, 1897 in Vienna, † January 25, 1969), who even described some of these species. Museum collections, including those like Vienna's, offer numerous advantages for taxonomic research. They provide significant cost savings by reducing the need for new field collections. Additionally, they grant access to rare or extinct species, contributing to the expansion of comprehensive geographic barcode databases (Hoban et al. 2022, Kress & Erickson 2012, Meusnier et al. 2008, Prosser et al. 2016). Crucially, these collections contain an abundance of taxonomic information gathered over time. By extracting genetic data from these extensively studied specimens, we can effectively bridge the gap between this existing taxonomic knowledge and newly collected specimens, via DNA barcoding.

Nevertheless, working with historical specimens, especially those previously fixed with formalin, presents challenges in obtaining complete COI barcodes due to DNA degradation (Baird et al. 2011). Formalin fixation can exacerbate these issues, leading to further fragmentation of DNA, base modifications like uracil and thymine derived from cytosine deamination, as well as various crosslinks, including protein-protein, protein-DNA, and interstrand DNA crosslinks (Do & Dobrovic 2015). These factors can complicate molecular analyses significantly. A possible solution lies in the use of short or minimalist barcodes, known as DNA mini-barcodes, spanning just 100-300 base pairs (Kress & Erickson 2012, Meusnier et al. 2008). These mini-barcodes significantly expand the applications of DNA barcoding and can be successfully obtained from even formalin-treated samples (Baird et al. 2011).

Another commonly used method for handling historical samples involves Next Generation Sequencing (NGS). NGS offers several potential benefits compared to Sanger sequencing. These include minimized amplification biases, the capability to process fragmented DNA, and maximizing the data obtained from historical samples (Prosser et al. 2016, Tin et al. 2014). Genome skimming is a high-throughput sequencing technique, involving shotgun sequencing of entire genomes without the need for specific target loci (Hoban et al. 2022). What's distinctive about genome skimming is its low coverage, often employed to save costs. However, this approach primarily generates data from the 'high-copy fraction,' which includes mitochondrial DNA (mtDNA) and ribosomal DNA. This method has potential for enhancing DNA barcode reference databases as it simultaneously generates data for commonly used barcoding markers across various taxa (Hoban et al. 2022).

4. Objectives of the Master's Thesis

In this master's thesis, three main objectives are pursued. These objectives collectively enhance our understanding of isopod taxonomy and diversity in Austria, while addressing the specific challenges associated with working on historical samples.

1. **Establishing a DNA Barcode Database**: The primary objective of this master's thesis is to create a DNA barcode database for terrestrial isopod species in Austria. This database utilizes the COI region, providing a molecular tool for species identification, overcoming the challenges posed by morphology-based identifications that often rely on male-specific characteristics.
2. **Identifying Cryptic Species**: The second objective involves applying phylogenetic methods and species delineation analyses to the generated COI sequences. This allows for the identification of potentially cryptic species within the isopod populations in Austria.
3. **Retrieving DNA Sequences from Historical Specimens**: The third objective centers on obtaining DNA sequences from historical isopod specimens, previously identified by

experts. This is accomplished through two distinct approaches: (1) amplifying mini-barcodes using Sanger sequencing and (2) conducting genome skimming through NGS. Various methods for library preparation are being explored and optimized under the genome skimming approach to create an effective library preparation workflow. These historical DNA sequences establish a direct connection between physical specimen vouchers and their DNA barcodes, thus bridging past and present taxonomic knowledge.

Materials and Methods

1. Preparation for Sanger Sequencing

1.1 Sample Collection and Preservation

Between June 2020 and July 2023, a total of 577 terrestrial isopod specimens were collected from various locations across all Austrian provinces, with primary contributions from Martin Schwentner, Stefan Koblmüller, and myself, among others. Sampling was conducted using a combination of hand picking and soil sieving. We attempted to collect specimens from different habitats such as forests, grasslands and urban areas to ensure a comprehensive representation of species diversity in Austria. Geographical coordinates were noted for each of the 65 collection sites. If possible, individuals were examined for the number of their tracheae, which are an important identification feature. However, they can only be clearly recognized on the living animal. We estimate that the number of animals counted for their trachea is around 50%. Individuals were then preserved in 80% ethanol to maintain the integrity of DNA.

1.2 DNA Extraction

A single leg was removed from each preserved isopod specimen using sterilized forceps to minimize contamination. The tissue samples were then transferred to sterile microcentrifuge tubes each of which contained 10 µl of GeneOn's Proteinase K and 90 µl ATL lysis buffer of The Qiagen DNeasy Blood and Tissue Kit. Samples were then incubated at 56°C for a few hours to ensure cell lysis and DNA release.

To purify the extracted DNA, magnetic beads were employed. 100 µl of AMPure XP Bead-Based Reagent from Beckman Coulter Life Sciences were added to the lysate mixture, followed by a 10-minute incubation step. The magnetic properties of the beads facilitated

their separation from the solution using a magnetic rack, enabling the removal of impurities and DNA purification.

Two washing steps were carried out using 180 µl of 80% ethanol to remove residual contaminants, and the purified DNA bound to the magnetic beads was eluted in 40 µl of nuclease-free H_2O. The eluted DNA was collected in a fresh microcentrifuge tube.

The extracted DNA samples were stored at -20°C until further analysis, ensuring their preservation for molecular applications, such as PCR amplification and sequencing.

Particularly small specimens were put whole into solution, and the remaining exoskeleton was preserved after digestion and converted to 80% ethanol for subsequent taxonomic identification. For this, incubation was performed for only 30 minutes.

1.3 PCR Amplification and DNA Barcoding

The cytochrome c oxidase subunit I (COI) gene, commonly used as a DNA barcode region for animal species, was specifically amplified by polymerase chain reaction (PCR). The first attempts were carried out by using the LCO1490/HCO2198 primer pair (5'-GGTCAACAAATCATAAAGATATTG-3'/5'-TAAACTTCAGGGTGACCAAAAAATCA-3') (Folmer et al. 1994) (Table 1). After the amplification of the first 48 samples I decided to continue with the QUIAGEN Multiplex PCR Kit as better results regarding positive PCR products were observed (Table 2). Successful amplification was confirmed by gel electrophoresis.

Table 1: COI PCR Amplification Parameters using Taq Polymerase

Note: DNA concentration varies across samples, and it is not known for all.

Reagent	x1 (µl)	
LCO1490 (10 mM)	1.5	PCR programm
HCO2198 (10 mM)	1.5	95°C 03:00

dNTP (25 mM each)	0.12	95°C	00:30	
$MgCl_2$ (25mM)	0.4	46°C	00:45	35x
10x PCR Buffer	1.5	72°C	01:00	
H_2O	7.9	72°C	05:00	
Taq Polymerase (5 U/µl)	0.075			
DNA	2			

Table 2: COI PCR Amplification Parameters using Multiplex MM

Note: DNA concentration varies across samples, and it is not known for all.

Reagent	x1 (µl)			
LCO1490 (10 mM)	1.5	PCR programm		
HCO2198 (10 mM)	1.5	95°C	15:00	
Multiplex MM	7.5	95°C	00:30	
H_2O	3	46°C	00:45	35x
DNA	1.5	72°C	01:00	
Σ	15	72°C	05:00	

1.4 Sample Selection for Amplification and Sequence Analysis of Nuclear Markers

To further investigate intraspecific divergence and the possible presence of cryptic species, two nuclear regions were chosen. The internal transcribed spacer 2 (ITS2) between the 5.8S and the 28S ribosomal RNA gene and a fragment of the 28S ribosomal RNA gene (28S) were amplified for a subset of samples. For this, three species with a particularly high intraspecific divergence based on my own sequence analysis were chosen: *Armadillidium vulgare*, *Trachelipus rathkii* and *Trachelipus ratzeburgii*. Within these species samples collected from various regions across Austria were selected to ensure representativeness. For the amplification of nuclear markers, the ITS2 and the 28S region were targeted using ITS3/ITS28 (5’-GCATCGATGAAGAACGCAGC-3’/5’-CGCCGTTACTAGGGGAATCCTTGTAAG-3’) (White et al. 1990/Wagstaff and Garnock-Jones 1998) primer pair or D1D2fw1/D1D2rev2

(5’-AGCGGAGGAAAAGAAACTA-3’/5’-ACGATCGATTTGCACGTCAG-3’) (Sonnenberg et al. 2007), along with DreamTaq DNA Polymerase by Thermo Scientific™ (Table 3). Again, gel electrophoresis was used to verify the success of the amplification.

Table 3: 28S/ITS2 PCR Amplification Parameters

Note: DNA concentration varies across samples, and it is not known for all.

Reagent	1x (µl)
forward Primer (10 mM)	1.5
reverse Primer (10 mM)	1.5
dNTPs (25 mM each)	0.3
10x DreamTaq Buffer	1.5
DreamTaq (5 U/µl)	0.05
H_2O	8.65
DNA	1.5

Due to the presence of indels, ITS2 region exhibited an excessive degree of diversity, making it challenging to obtain readable sequences for comparison. A similar challenge emerged with the 28S region, albeit to a lesser extent. Consequently, only two sequences per taxon remained viable for analysis. Hence, comparison of nuclear markers was not proceeded since the quantity of data was too small for a meaningful analysis.

1.5 Taxonomic Identification

Taxonomic identification was conducted by Martin Schwentner using the reverse taxonomy approach. This technique involves the initial grouping of specimens based on their molecular operational taxonomic units (MOTUs). Subsequently, individual specimens within each MOTU were identified using a taxonomic key provided by Schmölzer in 1965. This method proves effective for accurate species identification, particularly in cases where morphological identification is limited to male characteristics.

1.6 Sample Selection of Museum Specimen

The Natural History Museum of Vienna provided the source of historic specimens for the project. If possible I tried to integrate specimens including all Austrian species. Only animals collected in Austria and identified by Hans Strouhal were selected. In addition, animals collected before 1900 were prioritized to avoid potential fixation in formaldehyde, which could complicate molecular work due to issues like deamination of cytosine to uracil, crosslinks or single strand breaks. Finally, 80 individuals from 80 species or subspecies were selected for DNA extraction (Appendix A).

1.7 DNA Extraction of Museum Specimen

DNA extraction of all historical samples was performed in the clean room of the Natural History Museum Vienna. Through UV radiation and filter systems, this facility enables contamination-free DNA extraction, which is particularly important for museum material. The reaction process for historical samples was identical to that used for fresh samples (see Section 1.2). To account for the low DNA concentration in museum samples, a larger amount of tissue was utilized compared to the fresh material. However, this approach was undertaken cautiously to prevent any damage to the specimen, ensuring that morphological determination could still be pursued. Therefore, tissue was removed exclusively from only one side of the body along the sagittal plane leaving the second side intact. Body parts that represent important morphological characteristics, such as parts of the head and the last pair of legs, were also not removed. Here too, particularly small specimens were placed whole in solution to preserve the remaining exoskeleton after digestion. To compensate for the increased proportion of tissue, the amount of proteinase K and ATL lysis buffer was doubled. Samples were then incubated overnight at 56°C. This was followed by a magnetic beat-cleanup that is identical to the cleanup of the fresh samples, but with 300µl of magnetic beads. This represents 1.5x the amount of beads compared to the reaction solution. This

was expected to retain small DNA fragments as well. During the experimental process of establishing a workflow for processing these historical samples, elution volumes were successively adjusted, leading to variations.

1.8 PCR Amplification and DNA Barcoding of Museum Specimen

In the initial attempts to amplify historical COI barcodes, I had no success in obtaining full-length sequences. Consequently, the approach was shifted to focus on amplifying mini-barcodes, spanning 316 bp of the COI region. For this I employed the BR1 (5'-ACWGGWTGRACWGTNTAYCC-3') and BR2 (5'-TCDGGRTGNCCRAARAAYCA-3') primers (Elbrecht and Leese, 2017) with the QUIAGEN Multiplex PCR Kit (Table 4). Successful amplification was verified by gel electrophoresis.

Note that previous to PCR, samples were treated with a DNA repair reaction, detailed in Section 2.2 "Final Library Preparation Workflow", to address potential FFPE damage. To evaluate the effectiveness of the repair step, 21 samples and two extraction controls (K3.5 and K20.4) were subjected to two separate PCRs: one without and one with the FFPE repair.

Table 4. COI Mini-Barcodes PCR Reaction Parameters

Note: DNA concentration varies across samples, and it is not known for all.

Reagent	x1 (µl)			
BF1 (10 mM)	1.5	PCR programm		
BR2 (10 mM)	1.5	95°C	15:00	
Multiplex MM	7.5	95°C	00:30	
H_2O	3	46°C	00:45	35x
DNA	1.5	72°C	01:00	
Σ	15	72°C	05:00	

2. Data Analysis of Sanger Sequences

2.1 Sanger Sequence Processing and Alignment

The positive PCR products were subjected to bidirectional Sanger sequencing using the same PCR primers. Sequencing was performed by Macrogen's sequencing services. Quality check and editing of the resulting sequence data was performed utilizing Geneious R10.2 (https://www.geneious.com), thereby low-quality regions, primer sequences as well as ambiguous bases were manually trimmed or corrected. An outgroup, obtained from NCBI (https://www.ncbi.nlm.nih.gov/nuccore/MZ128370) was included. Geneious' alignment function was then used to align the processed sequences to each other. For this purpose, the multiple alignment algorithm MUSCLE was applied.

Using MEGA11: Molecular Evolutionary Genetics Analysis version 11 (Tamura, Stecher & Kumar 2021) software, I calculated a pairwise distance matrix and subsequently constructed a distance-based tree based on p-distances from the aligned sequences. This allowed an intermediate understanding of the genetic relationships of my dataset and a base for selecting individuals for nuclear marker amplification.

2.2 Phylogenetic Analysis

To further understand the evolutionary relationships among the isopod species studied, a Bayesian phylogenetic tree was constructed with MrBayes. This analysis involved employing Markov Chain Monte Carlo (MCMC) simulations, which served not only to establish the phylogenetic hypothesis represented by the tree's arrangement but also to calculate posterior probabilities, providing insights into the support for different branches. For reference, the outgroup, selected from NCBI data, was defined. The substitution model used for the DNA sequences was GTR+G+I, as suggested by the model selection function in

MEGA 11. The analysis was run for 50,000,000 generations. A tree was sampled every 5000 generations, with the first 1000 generations treated as burn-in. Additionally, six independent MCMC chains were run simultaneously to ensure convergence and robust results.

2.3 Species Delimitation

To investigate species delimitation, the aligned COI sequences were processed using the Assemble Species by Automatic Partitioning (ASAP) web server (Puilladre et al. 2001). ASAP is a species delimitation tool that relies on pairwise genetic distances to generate a list of partitions that are ranked based on a specific scoring system. This score is computed based on the probabilities of distinct species groups, considering both the barcode gap threshold and the distinctness of these groups.

Species delimitation was further explored by Generalized Mixed Yule Coalescent (GMYC) analysis which depends on detecting the transition between speciation to coalescence events within an ultrametric tree. Using BEAST 2.5 (Bouckaert et al. 2019) software, an ultrametric tree was created, with the General Time Reversible (GTR) model as the substitution model. To ensure a consistent evolutionary rate across branches, a strict clock was imposed. The Markov Chain Monte Carlo (MCMC) simulation incorporated a chain length of 10,000,000, and at each iteration, the parameters were stored at a storage frequency of 1,000. Additionally, the ingroup was predefined as monophyletic. Before running the GMYC analysis, I examined the trace panel using Tracer 1.7.1 (Rambaut et al. 2018) to ensure convergence.

3. Library Preparation for Next-Generation Sequencing (NGS)

3.1 Sample Selection

All museum samples extracted from the initial museum specimen selection (see Appendix A) were subjected to NGS library preparation based on their DNA quantity and quality. Both single-stranded (ssDNA) and double-stranded (dsDNA) measurements were performed using the Qubit fluorometer by Thermo Fisher Scientific (Qubit™ ssDNA Assay Kit and Qubit™ dsDNA Quantification Assay Kits). Note, that the ssDNA Assay Kit measures the concentration of both ssDNA and dsDNA. Due to an added step in the workflow, an attempt was made to convert ssDNA to dsDNA. This step was essential to account for the limitations inherent in common library preparation kits that only allow the use of dsDNA. Hence, if the amount of dsDNA was notably low and fell below the detection limit of the Qubit, samples were still included in subsequent steps of the NGS workflow, provided that there was a detectable amount of ssDNA. However, in instances where the amount of ssDNA fell below the detection limit, these samples were excluded from the subsequent workflow.

3.2 Final Library Preparation Workflow

The setup of the final DNA library preparation workflow involved a thoroughly designed process that includes several steps to improve the suitability of DNA extracts from historical museum specimens for NGS analysis. To address the challenges posed by degraded DNA, a series of strategic changes were made that resulted in a comprehensive workflow (Table 5).

The first step was performed using the NEBNext FFPE DNA Repair v2 module from New England BioLabs (Table 5, Section 1). This repair mix was specifically designed for the repair of formalin-fixed, paraffin-embedded (FFPE) samples. DNA extracts were incubated with a

mixture of enzymes according to the manufacturer's protocol with slight modifications. Notably, approximately one-third of the recommended sample volumes and reagent quantities were used in each case to accommodate the limited amount of DNA of historic museum specimens. This was followed by a purification process using magnetic beads, as described earlier.

To convert single-stranded DNA to double-stranded, a G-tailing procedure was employed, inspired by the method described by Tin et al. (2014) (Table 5, Section 2). In this process, samples are first heated to 96°C to separate complementary strands. Subsequently, deoxyguanosine triphosphates (dGTPs) are attached to single-stranded DNA, which in the next step serve as primer binding site for a primer consisting of six cytosine nucleotides. This facilitated the amplification of the second strand. dsDNA samples were once again purified using magnetic beads as described in previous steps.

The library preparation step encompassed two distinct approaches utilizing the NEBNext Ultra II FS DNA Library Prep Kit for Illumina (here: FS kit) and NEBNext Ultra II DNA Library Prep Kit for Illumina (here: Ultra II kit) from New England Biolabs. As shown in Section 3 of Table 5 both kits were employed according to the manufacturer’s protocol with the exception that for the FS library only one-third of the recommended sample and reagent volumes were employed whereas for Ultra II one-half of the volumes were used. A second exception to the protocol was made by employing Y-yoke adapters. The Y-yoke adapter serves two purposes: it facilitates the attachment of Illumina adapters while simultaneously integrating sample-specific barcodes or indices.

The FS Kit includes a fragmentation step that cuts fragments into specific lengths depending on the incubation time. Assuming that the DNA was already fairly fragmented, the incubation step was set to 10 minutes. The inclusion of the FS kit was motivated by the findings from the 4200 TapeStation System by Agilent, which indicated the presence of relatively long DNA fragments in some samples of approximately 1,500 bp.

A PCR was set up to amplify the library as well as to complete the Illumina adapters. It's important to note that the primers used in this step include an additional section that extends beyond the original primer binding site of the adapter. Notably, Illumina indices are incorporated into this section. Q5 High-Fidelity DNA Polymerase by New England Biolabs was used for this purpose (Table 5, Section 4). For each sample, two PCRs were conducted, which were pooled together in the subsequent beads clean-up process.

Table 5: Final Library Preparation Workflow.

Note: DNA concentration varies across samples (Appendix A: List of Museum Specimens and DNA Concentration).

1. FFPE Repair	
	1x (µl)
DNA	17
FFPE DNA Repair Buffer v2	2.333
FFPE DNA Repair Mix v2	0.666
15 min at 37°C Beads clean-up: 1.5x Beads. Elution in 20µl H_2O	
2. G-tailing	
2.1 Heat up	
15 min at 96°C	
2.2 G-tailing	
	1x (µl)
10x TdT Buffer	5
$CoCl_2$ (2.5 mM)	5
Terminale Transferase (20 U/µl)	0.5
dGTP (5mM)	1
DNA + H_2O	38.5
30 min at 37°C, 10 min at 70°C Beads clean-up: 1.5x Beads. Elution in 17µl H_2O	
2.3 C-Primer Binding and dsDNA Synthesis	
	1x (µl)
dNTP (10mM each)	4.5
10x NEBuffer	3

Klenow fragment (5 U/µl)	3
6C - Primer (15 mM)	3
DNA (G-tailed)	16.5
Beads clean-up: 1.5x Beads. Elution depending on library Kit used	
3. Library Preparation	
3. 1 FS - Library	
	1x (µl)
DNA	8.666
FS Reaction Buffer	2.333
FS Enzyme Mix	0.666
10 min at 27°C, 30 min at 65°C	
	1x (µl)
DNA (fragmented)	11.666
Ligation MM	10
Ligation Enhancer	0.333
Y-yoke adapter (1.5 µM)	0.833
15 min at 20°C Beads clean-up: 1x Beads. 17µl 0.1xTE Buffer	
3. 2 Ultra II – Library (alternative to 3.1 FS-library)	
	1x (µl)
Ultra II End Prep Enzyme Mix	1.5
Ultra II End Prep Reaction Buffer	3.5
DNA	25
30 min at 20°C, 30 min at 65°C	
Sample	30
Y-yoke adapter (1.5 µM)	1.25
Ultra II Ligation MM	15
Ligation Enhancer	0.5
15 min at 20°C Beads clean-up: 1.5x Beads. 10.5 µl H_2O	
4. PCR and Primer-binding for Illumina	
	1x (µl)
Q5 Polymerase	5
Primer (fw) (10 mM)	0.5
Primer (rv) (10 mM)	0.5
DNA	4
30 s at 98°C; 15 cycles: 10 s at 98°C, 1 min 15 s at 65°C; 5 min at 65°C Beads clean-up: 1x Beads. Elution in 17µl 0.1xTE Buffer	

3.3 Optimization Trials of aDNA

3.3.1 FFPE-Repair Trials

The effectiveness of the FFPE-repair process was evaluated on 21 samples, along with two extraction controls. These samples were subjected to the FFPE-repair procedure, as outlined in the final library preparation workflow (see Table 5, Section 1). Following this, a PCR amplification of mini-barcodes using the BF1 and BF2 primers (as indicated in Table 4) for both the repaired samples and the same samples without repair. Positive PCR products were confirmed through gel electrophoresis.

3.3.2 Library Preparation Trials

The success of each of the following trials was determined by an assessment of DNA quantity and/or quality. Qubit 4 Fluorometer, NanoDrop One/One^{C} Spektralphotometer by Thermo Scientific and TapeStation System were selectively employed based on the specific methods tested. By contrasting these measurements, I was able to identify a workflow that fits best to the aDNA samples.

The very first process of improving our library preparation method involved DNA extraction from the tissue of a freshly preserved *Pacifastacus leniusculus* (ID: 27931) from the museum collection. This approach was adopted to preserve the limited availability of museum specimens, particularly considering the small size of isopods, which inherently restricts the amount of extractable tissue. Moreover, this allowed us to systematically refine our methods without the problems associated with ancient DNA. Like the other extractions, the *P. leniusculus* tissue was digested by adding 180 µl of buffer and 20 µl of proteinase K and confining incubation at 56°C for several hours. This was followed by a beads clean-up process in which 200 µl beads were added. The washing steps correspond to those described above. To simulate highly fragmented ancient DNA, crayfish DNA was

subsequently digested by using New England Biolabs' restriction enzymes MSPI and EcoRI (Table 6).

Table 6: Parameters for Digestion of *P. leniusculus* DNA

Reagent	1x (µl)
10x Buffer	3
MSPI	0.3
EcoRI	0.3
H_2O	21.4
Crayfish DNA (64,2 ng/µl)	5

90 min at 37°C, 20 min at 10°C (temperature transition set to 1°C/s)

With the crayfish sample now fragmented, six distinct approaches (A-F) were formulated with the aim of optimizing G-tailing parameters (Table 7, Section 2). This was done to test and adjust critical factors for optimal results, taking into consideration the potential enzymatic reactions involved. For instance, the quantity of added dGTP was deliberately altered in these approaches. This variation was based on the fact that higher amounts of dGTP tend to enhance the efficiency of the Transferase enzyme, thereby creating longer G-tails. However, excessively long G-tails might be counterproductive. Thus, the adjustments in dGTP concentration were intended to fine-tune the G-tailing process. Furthermore, we examined the influence of the DNA to dGTP ratio. Approaches A-C utilized 16 µl of DNA (64,2 ng/µl), while D-F employed 5 µl, leading to variations in the DNA dGTP ratio (Table 7, Section 2). Based on the consistent and reliable results seen in the A-C subgroup, approaches D-F were deemed unnecessary for further investigation.

Further differentiation within the A-C approaches was introduced in the next step by modifying the type of C-Primers employed, characterized by varying lengths of cytosine nucleotides (6, 8, 10, or 15) (Table 7, Section 3). This variation resulted in the creation of distinct samples, each uniquely labeled as A6, A8, A10, B6, B8, B10, C6, C8, and C15. The cycler temperature settings were adjusted to each reaction approach.

Table 7: Parameters for Distinct G-tailing Trials

Note: The DNA concentration of the G-tailed DNA used in step 3 was not measured prior to the reaction and is therefore unknown.

1. Heat up					
15 min at 96°C					
2. G-Tailing					
Approach A	1x (µl)	Approach B	1x (µl)	Approach C	1x (µl)
10x TdT Buffer	5	10x TdT Buffer	5	10x TdT Buffer	5
$CoCl_2$ (2.5 mM)	5	$CoCl_2$ (2.5 mM)	5	$CoCl_2$ (2.5 mM)	5
Transferase (20 U/µl)	0.5	Transferase (20 U/µl)	0.5	Transferase (20 U/µl)	0.5
dGTP (5mM)	1	dGTP (5mM)	5	dGTP (5mM)	7.5
H_2O	22.5	H_2O	18.5	H_2O	16
DNA (64,2 ng/µl)	16	DNA (64,2 ng/µl)	16	DNA (64,2 ng/µl)	16
Σ	50	Σ	50	Σ	50
Approach D	1x (µl)	Approach E	1x (µl)	Approach F	1x (µl)
10x TdT Buffer	5	10x TdT Buffer	5	10x TdT Buffer	5
$CoCl_2$ (2.5 mM)	5	$CoCl_2$ (2.5 mM)	5	$CoCl_2$ (2.5 mM)	5
Transferase (20 U/µl)	0.5	Transferase (20 U/µl)	0.5	Transferase (20 U/µl)	0.5
dGTP (5mM)	0.3	dGTP (5mM)	1.6	dGTP (5mM)	2.4
H_2O	34.2	H_2O	32.9	H_2O	32.1
DNA (64,2 ng/µl)	5	DNA (64,2 ng/µl)	5	DNA (64,2 ng/µl)	5
Σ	50	Σ	50	Σ	50
30 min at 37°C, 10 min at 70°C Beads clean-up 1.5x Beads, A-C eluted in 60 µl H_2O, D-F in 30 µl H_2O					
3. PCR with C-Primer (dsDNA Synthesis)					
	1x (µl)	Sample		Cycler	
dNTP (10 mM each)	1.5	A6, A8, B6, C6, C8		180 min at 22°C, 20 min at 75°C	
10x NEBuffer	1	A10, B10, C10		30 min at 39°C, 20 min at 75°C	
Klenow (5U/ µl)	1	C15		30 min at 62°C, 20 min at 75°C	
Primer (15 mM)	1				
DNA (G-tailed)	5.5				

Next, the ligation of adapters for Illumina was tested by employing the Ultra II Kit (see Table 5, Section 3.2). The process includes an initial step designed to blunt-end and A-tail the now double-stranded DNA. This phase was established to enable adapter ligation in the subsequent step. However, the Klenow fragment, which was employed in the previous G-tailing step, can be used for this exact process. We therefore tested an alternative ligation

approach by employing T4 Ligase by New England Biolabs directly after the PCR of the G-tailing process (Table 8) instead of relying on a specific kit. Both approaches were tested on samples A6, A8, B8 and B10. Reaction parameters for Ultra II Library Prep are stated in the final workflow chapter. The effectiveness of the various tests was assessed based on the quantity of dsDNA measured using the Qubit fluorometer.

Table 8: Parameters for T4 Ligation Reaction

Note: DNA concentration among samples ranges from 2,72 to 4,84 ng/µl.

T4 Ligation Reaction	
Beads clean-up previous to reaction: 1.2x Beads, eluted in 17 µl H_2O	
	1x (µl)
10x T4 Ligase Reation Buffer	3
T4 DNA Ligase	1
Y-yoke adapter (1.5 µM)	3
DNA (post G-tailing)	15
H_2O	8
60 min at 22°C, 10 min at 65°C, 1 min at 10°C (second temperature transition set to 1°C/s) Beads clean-up: 1x Beads, eluted in 17 µl H_2O	

3.4 DNA Quantification, Selection, and Illumina Sequencing

To quantify DNA content within my final library DNA concentration, again, Qubit 4 Fluorometer was employed. We set a minimum concentration threshold of 2 ng/µl. Samples with lower concentrations were excluded from further sequencing. This was followed by a sample pooling, where the volume of each sample was adjusted according to their respective concentrations of a 250 - 600 bp size range. The concentration of this region was measured with the TapeStation System. Consequently, we obtained a pool of libraries with approximately similar DNA concentrations of each library, according to TapeStation measurement.

However, when assessing the size distribution, certain samples exhibited a considerable portion of relatively large fragments, estimated to be around 1,500 bp in length. To account

for this observation and mitigate potential adapter or primer dimer interference, a size range of 250 to 600 bp was targeted for accurate DNA fragment selection. This selection was performed using Sage Science's BluePippin DNA Size Selection System to ensure optimal preparation of DNA fragments for subsequent Illumina sequencing. Despite subsequent attempts from Martin Schwentner to excise the size range of interest manually from gel electrophoresis and Tricia Goulding's attempt to filter out oversized fragments by adjusting the volume of beads during a beads clean-up procedure, TapeStation analysis still indicated the persistence of these large fragments. The conclusion was subsequently reached that the observation could be due to problems within the TapeStation system itself.

4. Analysis of Illumina Data

The Illumina sequencing process was collaboratively undertaken together with Tricia Goulding with the sequencing service provider Genohub.

The analysis of Illumina data sequences was conducted by Martin Schwentner, utilizing the MitoFinder (Allio et al. 2020). This tool facilitated the extraction of mitochondrial DNA sequences from the acquired genomic sequencing data. To identify COI sequences the mitochondrial contigs derived from MitoFinder from each individual were submitted to a BLAST search. However, these sequences were not included in the final phylogenetic analysis. This omission was a result of the delay in submitting the sequences to the sequencing service provider, which stemmed from extensive efforts made to address library discrepancies arising from errors in the TapeStation analysis.

Results

1. Phylogenetic analysis and Species Delimitation

The final dataset comprises 342 COI sequences, including 15 museum specimens. As an outgroup, I incorporated a sequence from *Disparella sp.*, a species belonging to the Asellota suborder of Isopoda. Note that the full phylogeny of isopods remains unresolved, so I cannot definitively confirm that Asellota represents the sister group of Oniscidea. It comprises 552 sites in total, with 333 of these being variable. It is important to highlight that the dataset inadvertently includes two *Gammarus* and one *Daphnia* sequences due to shared sequencing submission. These three sequences, along with the outgroup sequence, will not be considered in subsequent analyses unless explicitly stated otherwise. Additionally, six sequences have accidental duplicates (Figure 1). These duplicates will be treated as single sequences in the analyses. These errors persisted in phylogenetic analysis due to time constraints. Furthermore, the dataset encompasses three sequences from *Asellus aquaticus*, which belongs to the family Asellota and is aquatic rather than terrestrial. However, these sequences will still be considered as they are part of the Austrian isopod fauna. The analysis thereby consists of 317 newly generated sequences belonging to 30 morphologically identified species from eleven families (Table 9).

Table 9: Species with Morphological Determinations, Sequence Counts and Families.

Note: Sequence counts are shown in brackets. In instances where species identification was unattainable, only the genus, 'sp.,' or the family name is provided.

Family	Species	
Agnaridae	*Protracheoniscus* sp.	(1)
	Protracheoniscus politus	(39)
Armadillidiidae	*Armadillidium vulgare*	(51)
	Armadillidium sp.	(2)
	Armadillidium opacum	(1)
	Armadillidium versicolor	(4)

Asellidae	*Asellus aquaticus*	(3)
Cylisticidae	*Cylisticus convexus*	(15)
Ligiidae	*Ligidium germanicum*	(10)
	Ligidium cf. *germanicum*	(5)
	Ligidium hypnorum	(4)
Oniscidae	*Oniscus asellus*	(2)
Philosciidae	*Lepidoniscus minutus*	(15)
	Philoscia muscorum	(3)
	Philoscia affinis	(10)
Platyarthridae	*Platyarthrus hoffmannseggii*	(2)
Porcellionides	*Porcellionides pruinosus*	(3)
	Porcellio spinicornis	(8)
	Porcellio scaber	(16)
Trachelipodidae	*Porcellium collicola*	(16)
	Porcellium conspersum	(2)
	Trachelipus rathkii	(34)
	Trachelipus ratzeburgii	(34)
Trichoniscidae	*Hyloniscus riparius*	(24)
	Haplophthalmus mengii	(1)
	Haplophthalmus danicus	(7)
	Trichoniscus sp.	(1)
	Trichoniscus pusillus	(2)
	Trichoniscidae A	(1)
	Trichoniscidae B	(1)

The ASAP partition with the highest asap-score (ASAP1) resulted in the delineation of 39 putative species (including 34 terrestrial Isopoda) and a threshold distance of 0.12 (Figure 1). The ASAP partition with the second highest score (ASAP2) identified 44 putative species (including 39 terrestrial Isopoda) at a threshold distance of 0.06. For the subsequent discussion, I will focus on these two ASAP partitions.

The GMYC analysis revealed the presence of 56 putative species (including 51 terrestrial Isopoda) within the dataset, with a threshold time at - 0.03 (Figure 1).

In the Bayesian phylogenetic analysis (Figure 1), all morphologically identified species were observed to form monophyletic groups. Notably, the posterior probability support for the majority of these species exceeded 99%. However, *Platyarthrus hoffmannseggii* exhibited lower posterior probability support.

At the family level, the phylogenetic analysis (Figure 1) reveals that several families do not form monophyletic groups. Among the eleven represented families, at least five, including Trachelipodidae, Trichoniscidae, Philosciidae, Porcellionidae, and Armadillidiidae, are not monophyletic. In many cases, there are low support values, which indicate that there is not sufficient data to resolve the topology. However, the Ligiidae family forms a well-supported monophyletic group.

Specifically, all three Philosciidae species clustered together with *Oniscus asellus* (Oniscidae), forming one clade. Trichoniscidae B (Trichoniscidae) and *Porcellio laevis* (Porcellionides) are also grouped with this clade. Within the Trichoniscidae family, some species cluster with *Asellus aquaticus* (Asellota) and *Platyarthrus hoffmannseggii* (Platyarthridae). The Porcellionides family displayed multiple splits. *Porcellionides pruinosus* and *Porcellio spinicornis* were clustered together, separate from *Porcellio scaber,* which formed a clade with *Armadillidium pictum* (Armadillidiidae). The final split within Porcellionides resulted in a clade consisting of *Porcellium collicola* and *P. consersum*, forming a sister group to the Agnaridae family. All putative species within Trachelipodidae formed a clade, although *Armadillidium nasatum* (Armadillidiidae) was also within this clade.

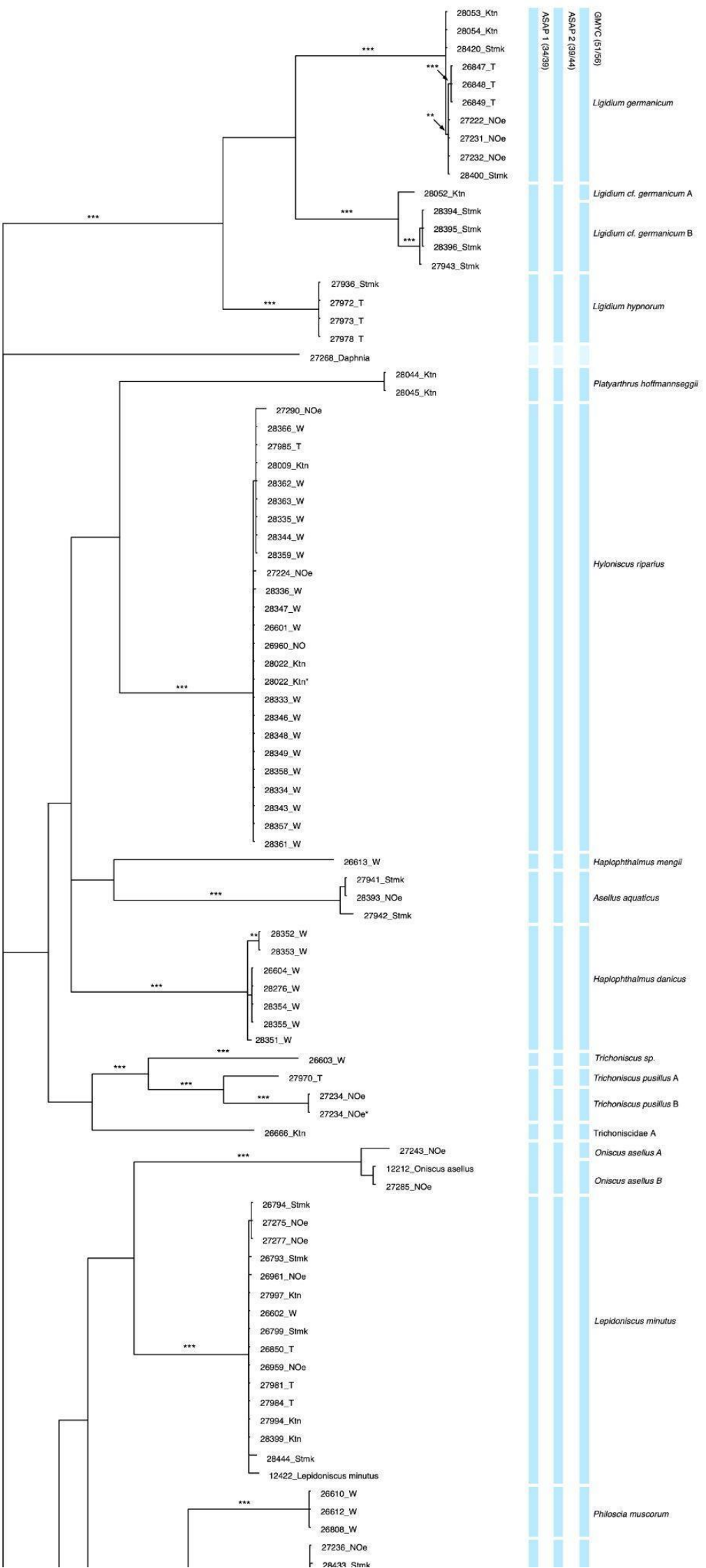
ASAP 1 (34/39)
ASAP 2 (39/44)
GMYC (51/56)
28053_Ktn
28054_Ktn
28420_Stmk
26847_T
26848_T
26849_T
27222_NOe
27231_NOe
27232_NOe
28400_Stmk
Ligidium germanicum
28052_Ktn
28394_Stmk
28395_Stmk
28396_Stmk
27943_Stmk
Ligidium cf. germanicum A
Ligidium cf. germanicum B
27936_Stmk
27972_T
27973_T
27978_T
Ligidium hypnorum
27268_Daphnia
28044_Ktn
28045_Ktn
Platyarthrus hoffmannseggii
27290_NOe
28366_W
27985_T
28009_Ktn
28362_W
28363_W
28335_W
28344_W
28359_W
27224_NOe
28336_W
28347_W
26601_W
26960_NO
28022_Ktn
28022_Ktn*
28333_W
28346_W
28348_W
28349_W
28358_W
28334_W
28343_W
28357_W
28361_W
Hyloniscus riparius
26613_W
Haplophthalmus mengii
27941_Stmk
28393_NOe
27942_Stmk
Asellus aquaticus
28352_W
28353_W
26604_W
28276_W
28354_W
28355_W
28351_W
Haplophthalmus danicus
26603_W
Trichoniscus sp.
27970_T
Trichoniscus pusillus A
27234_NOe
27234_NOe*
Trichoniscus pusillus B
26666_Ktn
Trichoniscidae A
27243_NOe
12212_Oniscus asellus
27285_NOe
Oniscus asellus A
Oniscus asellus B
26794_Stmk
27275_NOe
27277_NOe
26793_Stmk
26961_NOe
27997_Ktn
26602_W
26799_Stmk
26850_T
26959_NOe
27981_T
27984_T
27994_Ktn
28399_Ktn
28444_Stmk
12422_Lepidoniscus minutus
Lepidoniscus minutus
26610_W
26612_W
26808_W
Philoscia muscorum
27236_NOe
28433_Stmk

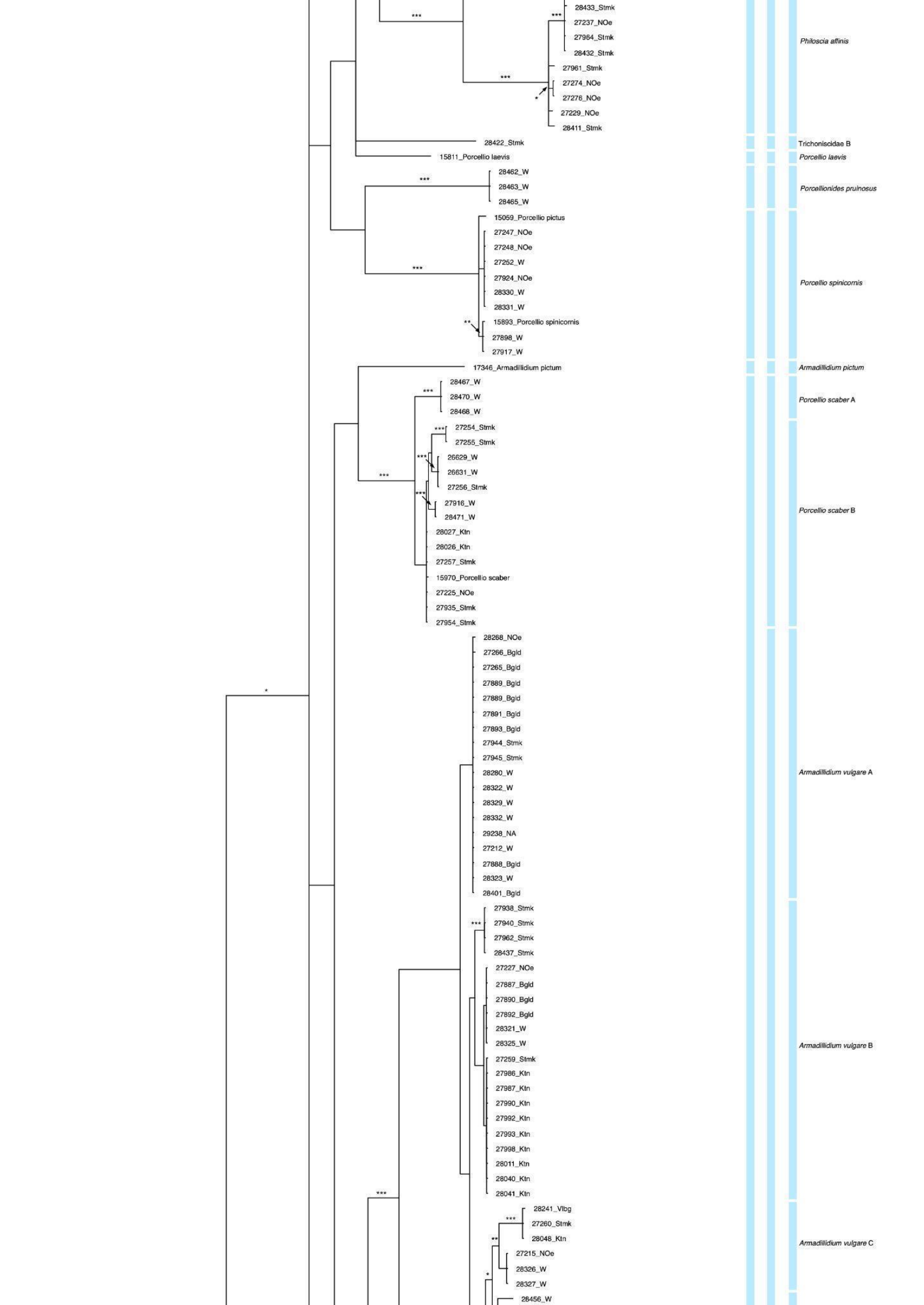
28433_Stmk
27237_NOe
27964_Stmk
28432_Stmk
27961_Stmk
27274_NOe
27276_NOe
27229_NOe
28411_Stmk
Philoscia affinis
28422_Stmk
Trichoniscidae B
15811_Porcellio laevis
Porcellio laevis
28462_W
28463_W
28465_W
Porcellionides pruinosus
15059_Porcellio pictus
27247_NOe
27248_NOe
27252_W
27924_NOe
28330_W
28331_W
15893_Porcellio spinicornis
27898_W
27917_W
Porcellio spinicornis
17346_Armadillidium pictum
Armadillidium pictum
28467_W
28470_W
28468_W
Porcellio scaber A
27254_Stmk
27255_Stmk
26629_W
26631_W
27256_Stmk
27916_W
28471_W
28027_Ktn
28026_Ktn
27257_Stmk
15970_Porcellio scaber
27225_NOe
27935_Stmk
27954_Stmk
Porcellio scaber B
28268_NOe
27266_Bgld
27265_Bgld
27889_Bgld
27889_Bgld
27891_Bgld
27893_Bgld
27944_Stmk
27945_Stmk
28280_W
28322_W
28329_W
28332_W
29238_NA
27212_W
27888_Bgld
28323_W
28401_Bgld
Armadillidium vulgare A
27938_Stmk
27940_Stmk
27962_Stmk
28437_Stmk
27227_NOe
27887_Bgld
27890_Bgld
27892_Bgld
28321_W
28325_W
27259_Stmk
27986_Ktn
27987_Ktn
27990_Ktn
27992_Ktn
27993_Ktn
27998_Ktn
28011_Ktn
28040_Ktn
28041_Ktn
Armadillidium vulgare B
28241_Vlbg
27260_Stmk
28048_Ktn
27215_NOe
28326_W
28327_W
28456_W
Armadillidium vulgare C

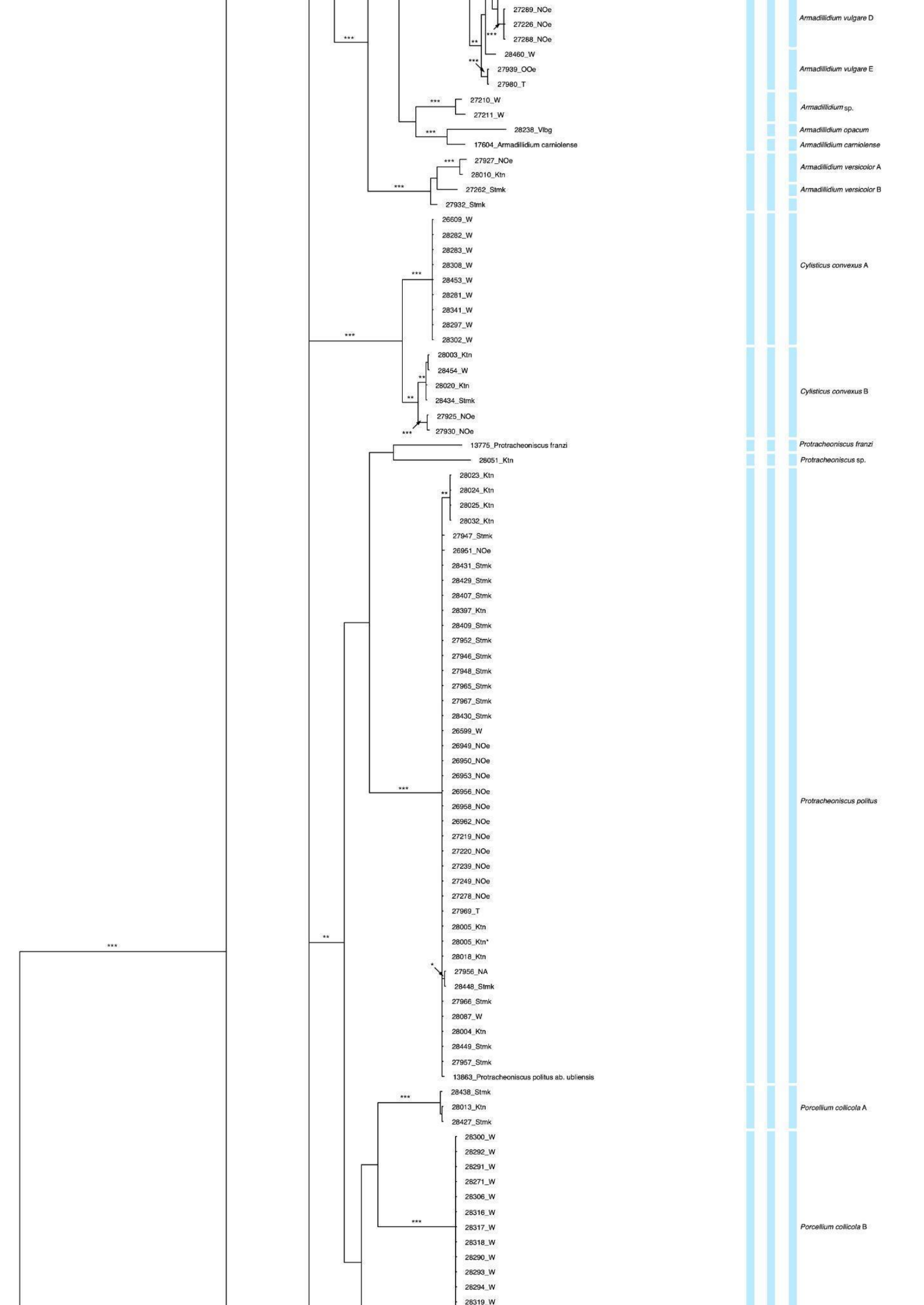
27289_NOe
27226_NOe
27288_NOe
28460_W
27939_OOe
27980_T
Armadillidium vulgare D
Armadillidium vulgare E
27210_W
27211_W
Armadillidium sp.
28238_Vlbg
Armadillidium opacum
17604_Armadillidium carniolense
Armadillidium carniolense
27927_NOe
28010_Ktn
27262_Stmk
27932_Stmk
Armadillidium versicolor A
Armadillidium versicolor B
26609_W
28282_W
28283_W
28308_W
28453_W
28281_W
28341_W
28297_W
28302_W
Cylisticus convexus A
28003_Ktn
28454_W
28020_Ktn
28434_Stmk
27925_NOe
27930_NOe
Cylisticus convexus B
13775_Protracheoniscus franzi
28051_Ktn
Protracheoniscus franzi
Protracheoniscus sp.
28023_Ktn
28024_Ktn
28025_Ktn
28032_Ktn
27947_Stmk
26951_NOe
28431_Stmk
28429_Stmk
28407_Stmk
28397_Ktn
28409_Stmk
27952_Stmk
27946_Stmk
27948_Stmk
27965_Stmk
27967_Stmk
28430_Stmk
26599_W
26949_NOe
26950_NOe
26953_NOe
26956_NOe
26958_NOe
26962_NOe
27219_NOe
27220_NOe
27239_NOe
27249_NOe
27278_NOe
27969_T
28005_Ktn
28005_Ktn*
28018_Ktn
27956_NA
28448_Stmk
27966_Stmk
28087_W
28004_Ktn
28449_Stmk
27957_Stmk
13863_Protracheoniscus politus ab. ubliensis
Protracheoniscus politus
28438_Stmk
28013_Ktn
28427_Stmk
Porcellium collicola A
28300_W
28292_W
28291_W
28271_W
28306_W
28316_W
28317_W
28318_W
28290_W
28293_W
28294_W
28319_W
Porcellium collicola B

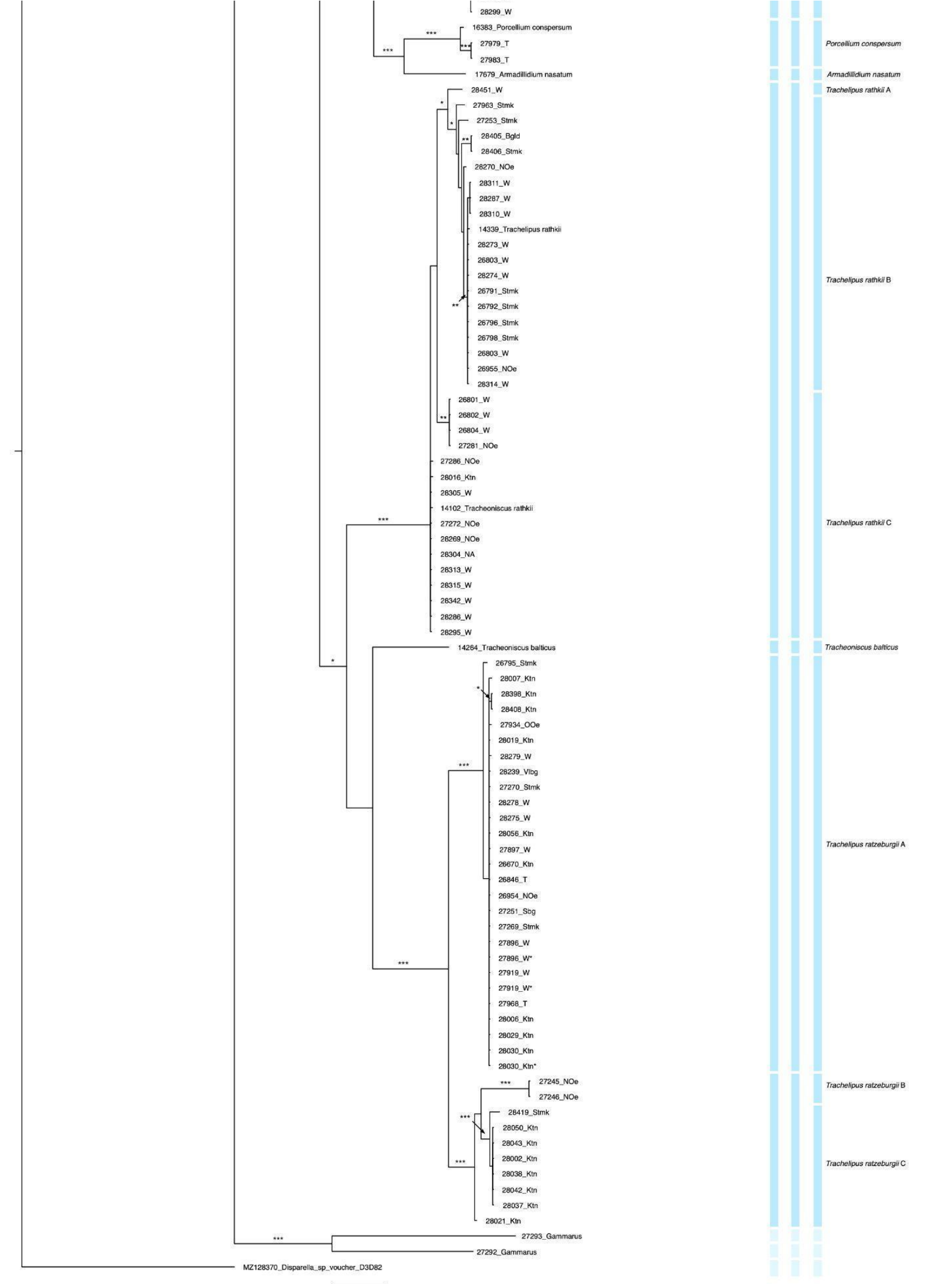
28299_W
16383_Porcellium conspersum
27979_T
27983_T
17679_Armadillidium nasatum
28451_W
27963_Stmk
27253_Stmk
28405_Bgld
28406_Stmk
28270_NOe
28311_W
28287_W
28310_W
14339_Trachelipus rathkii
28273_W
26803_W
28274_W
26791_Stmk
26792_Stmk
26796_Stmk
26798_Stmk
26803_W
26955_NOe
28314_W
26801_W
26802_W
26804_W
27281_NOe
27286_NOe
28016_Ktn
28305_W
14102_Tracheoniscus rathkii
27272_NOe
28269_NOe
28304_NA
28313_W
28315_W
28342_W
28286_W
28295_W
14264_Tracheoniscus balticus
26795_Stmk
28007_Ktn
28398_Ktn
28408_Ktn
27934_OOe
28019_Ktn
28279_W
28239_Vbg
27270_Stmk
28278_W
28275_W
28056_Ktn
27897_W
26670_Ktn
26846_T
26954_NOe
27251_Sbg
27269_Stmk
27896_W
27896_W*
27919_W
27919_W*
27968_T
28006_Ktn
28029_Ktn
28030_Ktn
28030_Ktn*
27245_NOe
27246_NOe
28419_Stmk
28050_Ktn
28043_Ktn
28002_Ktn
28038_Ktn
28042_Ktn
28037_Ktn
28021_Ktn
27293_Gammarus
27292_Gammarus
MZ128370_Disparella_sp_voucher_D3D82
0.06
Porcellium conspersum
Armadillidium nasatum
Trachelipus rathkii A
Trachelipus rathkii B
Trachelipus rathkii C
Tracheoniscus balticus
Trachelipus ratzeburgii A
Trachelipus ratzeburgii B
Trachelipus ratzeburgii C

Figure 1: Bayesian Phylogenetic Tree with Species Delimitation Boundaries and Morphological Species Identifications

Vertical bars indicate putative species delimitations of different analyses. The numbers in parentheses adjacent to the species delimitation analysis indicate the total number of putative species considering the entire dataset (including the outgroup and non-isopod sequences), as well as the number of only terrestrial putative isopod species. The species names correspond to morphological identifications, which are partly supported by genetic identifications. Species that have been subdivided into groups A, B, C, etc., correspond to the delimitation analysis with the highest degree of splitting. Duplicates are labeled with an asterisk (*). Gammarus *and* Daphnia *sequences are indicated as such. Sequences from museum specimens are labeled with their original identifications by Hans Strouhal. Note that the current nomenclature differs from the original identifications in some instances:* Porcellio pictus *(SYN)* = **P. spinicornis**, Trachelipus balticus *(SYN)* = **T. nodulosus**. Porcellio politus ubliensis *is currently accepted as* **P. ubliensis**, *however, morphological determinations rather suggest* **P. politus**. *Posterior Probability ≥ 99 indicated as '***', ≥ 95 indicated as '**', and ≥ 90 indicated as '*'.*

Most species exhibited a maximum intraspecific distance below 6%, with *Armadillidium vulgare* (6.5%) and *Cylisticus convexus* (6.3%) slightly exceeding this threshold (Table 10; Appendix B). Certain putative species exhibited remarkably high intraspecific distances, including *Porcellium collicola* (13.9%), *Trachelipus ratzeburgii* (10.4%), and *Tracheoniscus pusillus* (11.7%) .

Table 10: Range of Intraspecific p-Distances within Morphological Species

Note: in cases where only one sequence is available per species, no range is provided.

Species	Intraspecific pairwise distance (min-max) (%)	Nr. of Individuals
Armadillidium sp.	1.8	2
Armadillidium carniolense		1
Armadillidium nasatum		1
Armadillidium opacum		1
Armadillidium pictum		1
Armadillidium versicolor	0-5.4	3

Armadillidium vulgare	0-6.5	51
Asellus aquaticus	0-1.6	3
Cylisticus convexus	0-6.3	15
Hypophthalmus danicus	0-1.7	7
Haplophthalmus mengii		1
Hyloniscus riparius	0-1.4	25
Lepidoniscus minutus	0-1.4	16
Ligidium cf. *germanicum*	0-3.8	5
Ligidium germanicum	0-0.4	10
Ligidium hypnorum	0	4
Oniscus asellus	0-4.1	3
Philoscia affinis	0-3.1	10
Philoscia muscorum	0	3
Platyarthrus hoffmannseggii	0	2
Porcellio laevis		1
Porcellio scaber	0-5.8	17
Porcellio spinicornis	0-1.8	10
Porcellionides pruinosus	0	1
Porcellium collicola	0-13.9	16
Porcellium conspersum	0-1.2	3
Protracheoniscus franzi		1
Protracheoniscus politus	0-1.3	41
Protracheoniscus sp.		1
Trachelipus nodulosus		1
Trachelipus rathkii	0-5.4	36
Trachelipus ratzeburgii	0-10.4	27
Trichoniscidae (26666)		1
Trichoniscidae (28422)		1
Trichoniscus pusillus	0-11.7	3
Trichoniscus sp.		1

2. Historic Samples

Out of the 80 selected museum specimens (Appendix A), we successfully obtained COI sequences from 17 specimens using two different approaches (Appendix A, Table 11).

From the initial set of 33 submitted for Illumina sequencing (Appendix A, Table 15), ten libraries were found to include mitochondrial DNA as identified by MitoFinder. Among these ten libraries, four were found to contain the COI DNA barcoding region. These samples were labeled as 17604, 9682, and two libraries from 15059, both generated with the FS Kit, with one library undergoing the G-tailing procedure and the other not. Sample 17604 notably provided the complete mitochondrial genome (Appendix A, Table 11).

From 15 specimens a 316 bp long fragment of the COI DNA barcoding region was amplified and sequences were generated through Sanger sequencing (Appendix A, Table 11). All sequences obtained through Illumina sequencing could also be acquired through Sanger sequencing, with the exception of 9682. Upon comparing sequences generated by both Sanger and Illumina sequencing methods, no differences were observed.

The genetic analysis substantiated the accuracy of most museum specimen identifications, aligning with established references. However, one exception arose concerning a specimen initially designated as *Protracheoniscus politus* ab. *ubliensis*. While this suborder was once considered a subspecies of *P. politus*, it has since been recognized as a distinct species, *P. ubliensis*. Genetic and morphological evidence conclusively classified our specimen under *P. politus.*

Table 11: COI (Mini-)Barcode Sequences Generated from Museum Specimens and Applied Sequencing Methods.

Note: 'x' indicates that at least a part of the COI barcoding region could be generated with the corresponding sequencing method. The current nomenclature differs from the original identifications in some instances: Porcellio pictus *(SYN)* = **P. spinicornis**, Trachelipus balticus *(SYN)* = **T. nodulosus***,* Porcellio politus ubliensis *is currently accepted as* **P. ubliensis***, however, morphological determinations rather suggest* **P. politus***.*

ID	Species	Illumina	Sanger
9682	*Hyloniscus riparius*	x	
12212	*Oniscus asellus*		x
12422	*Lepidoniscus minutus*		x

13775	*Protracheoniscus franzi*		x
13863	*Protracheoniscus politus* ab. *ubliensis*		x
14102	*Tracheoniscus rathkii*		x
14264	*Tracheoniscus balticus*		x
14339	*Trachelipus rathkii*		x
15059	*Porcellio pictus*	x	x
15811	*Porcellio laevis*		x
15893	*Porcellio spinicornis*		x
15970	*Porcellio scaber*		x
16383	*Porcellium conspersum*		x
17346	*Armadillidium pictum*		x
17604	*Armadillidium carniolense*	x	x
17679	*Armadillidium nasatum*		x

In the NGS sequencing results, it's important to note a variation in the number of reads per library (Table 12). These differences stem from issues during the TapeStation measurement, where a significant portion of larger fragments persisted even after attempts to isolate the 250-600 bp size range. Consequently, the subsequent volume adjustments of each sample based on these measurements were inaccurate. In addition, the number of reads is significantly lower when primers are removed(Table 12). This indicates that a considerable portion of the sequenced material consisted of primer sequences.

Table 12: Museum Specimen Library Overview Read Counts per Library

Codes: 'x' indicates employed library preparation methods. Excluded samples are marked with an asterisk (*). Samples with COI sequences are indicated in bold. Rp = read pairs.

ID	FFPE-Repair	G-Tailing	Kit	Total Rp	Rp without primers	Difference in Rp
12196	x	x	FS	510738	20510	490228
12212	x		Ultra II	647606	78839	568767
12212	x	x	Ultra II	709591	17043	692548
12234	x		Ultra II	383735	272828	110907
12234	x	x	Ultra II	2817539	6077	2811462
12422	x	x	FS	1601729	1383154	218575

12786	x	x	FS	1723599	226717	1496882
13125	x		FS	13717706	12911144	806562
13125			FS			
13133	x		FS	41047648	39626244	1421404
13133*			FS			
13863	x	x	FS	976230	460222	516008
13917	x	x	FS	675265	41533	633732
13945*	x	x	Ultra II			
14102	x	x	Ultra II	7438541		7438541
14367	x	x	FS	3082405	93003	2989402
14401	x	x	FS	1299852	508650	791202
14958	x	x	FS	882828	16984	865844
15059	x		Ultra II	2988945	541197	2447748
15059	**x**	**x**	**FS**	**2221738**	**1153277**	**1068461**
15059	**x**		**FS**	**47339380**	**44251370**	**3088010**
15504	x	x	FS	804342	637342	167000
15511	x	x	Ultra II	4700326	8136	4692190
15811	x	x	Ultra II	17111788	4625694	12486094
16057	x		Ultra II	84926984	64444043	20482941
16057	x	x	Ultra II	2470989	13115	2457874
16299	x	x	FS	14003823	11159367	2844456
16383	x	x	FS	2042490	1856158	186332
16964	x	x	FS	1258249	39873	1218376
17346	x	x	FS	1374139	172371	1201768
17604	**x**	**x**	**FS**	**859226**	**770226**	**89000**
17628	x	x	FS	1748290	90347	1657943
22134*	x	x	FS			
8841*	x	x	FS			
9611	x	x	FS	2972488	971275	2001213
9682	**x**	**x**	**FS**	**30208122**	**23061145**	**7146977**
9711	x	x	FS	1590388	1386312	204076

2.1 Optimization Trials of aDNA

2.3.1 FFPE-Repair Trials

The assessment of the efficacy of FFPE repair encompassed 21 samples and two extraction controls (Table 13). Among these, four PCR products of the short COI fragment yielded positive PCR results in the absence of the FFPE repair procedure. These same four samples, plus three additional samples exhibited positive PCR products when subjected to FFPE repair. Sample 11334 initially displayed a positive PCR product during electrophoresis but was excluded from further analysis during the editing process due to its low quality. Samples 12422, 13863, 15059, and 17346 exhibited no discernible differences when comparing each sequence with and without repair (Table 13). Notably, in the case of sample 17346 a single nucleotide exhibited dual signals for both ‘C’ and ‘T’. This was observed in both sequences, one with FFPE repair and one without. The sequence of sample 16383 was of bad quality, with only 171 bp of each sequence being usable. Similarly, for 17679 a usable sequence of 240 bp was obtained.

All sequences obtained were compared to corresponding sequences from fresh specimens of the same species, when available, in order to find potential mutations that may have arisen due to formol damage (Table 13). However, no discrepancies were observed.

Table 13: Outcome of FFPE-Repair Trial Evidenced by Positive PCR Amplification of the Mini-Barcode Sequences

DNA concentration of the Extracted DNA was measured using Qubit Fluorometer. ‘x’ indicates a positive PCR result.

Museum ID	Year of Collection	DNA (ng/ul)	PCR with FFPE-Repair	PCR without FFPE-Repair
K20.4	-	-		
K3.5	-	-		
8866	1952	0.3		
8929	1967	Too low		

9092	1963	0.7		
9123	1938	Too low		
9151	1947	0.58		
9201	1946	0.54		
9474	1948	0.34		
11334	1963	1.4		
11499	1951	0,146		
12422	1952	11.2	x	x
12862	1947	0.82		
13775	1952	2.02	x	
13863	1890	11.1	x	x
14945	1896	1.53		
14958	1894	16.4		
15059	1887	27.2	x	x
16163	1946	6.88		
16192	1946	1.82		
16383	1961	15.6	x	
16942	1890	0.6		
17346	1894	10.3	x	x
17679	1946	0.6	x	

2.3.2 Library Preparation Trials

The G-Tailing trials encompassed six distinct approaches (A-F; see Table 7,3.3.2.), using DNA from the same individual of *P. leniusculus,* each including different DNA to dGTP ratios. Among these, approaches A-C underwent additional differentiation through the usage of different C-Primers, indicated by the numbers 6 and 8. Among identical primer sets, approach B consistently yielded the highest concentration (Table 14). Due to the relatively consistent DNA concentrations, ranging from 2.25 ng/µl (C6) to 4.84 ng/µl (B10), a decision was made to exclude approaches D-F from further investigations. This decision reflected the extensive approaches already tested and the overall positive results obtained in the tests A-C. Hence, subsequent trials focused on A6, A8, B8, and B10 due to their elevated dsDNA concentrations compared to C.

Table 14: Pre-PCR DNA Concentrations Obtained from G-Tailing Trials

Note: The numbers 6 and 8 indicate the count of cytosine nucleotides of a C-Primer. Letters A-C correspond to different DNA to dGTP ratio variations employed.

Sample	ng/µl
A6	3.22
B6	3.18
C6	2.26
A8	2.72
B8	3.04
C8	2.32
A10	3.68
B10	4.84
C10	3.38
C15	2.62

Two distinct approaches regarding the adapter ligation were used: first, direct ligation with the T4 Ligase which yielded undetectable DNA concentrations after PCR for all four samples according to Qubit fluorometer measurements (Table 15). Second using the Ultra II Kit, which resulted in relatively consistent DNA concentrations after PCR, varying from 17.9 ng/µl (A6) to 14.8 ng/µl (B8). Consequently, I decided to proceed with the A6 approach combined with the Ultra II Kit for the final library preparation workflow of the historical isopod DNA. However, due to the presence of relatively large fragments in the libraries, as assessed by Tapestation, I also tried the FS kit which includes a fragmentation step to address this issue.

Table 15: Post-PCR DNA Concentrations of Samples Selected for Adapter Ligation Trials

Note: The numbers 6-10 indicate the count of cytosine nucleotides of a C-Primer. Letters A and B correspond to different DNA to dGTP ratio variations employed.

Sample	Approach	ng/µl
A6	T4	Too low
A8	T4	Too low
B8	T4	Too low

B10	T4	Too low
A6	Ultra II	17.9
A8	Ultra II	15.2
B8	Ultra II	14.8
B10	Ultra II	15.9

Out of the initial 80 selected museum specimens, 37 samples underwent the library preparation process, due to low DNA concentrations in the remaining samples (Table 16). However, four samples were later excluded from Illumina sequencing due to insufficient DNA content in the final library in the 250-600 bp size range. It’s important to note that the concentrations of samples 13945, 14102, 15511, 15911, 15057, 12234, 12212, and 15059 (Table 16) are not directly comparable with each other due to variations in elution volumes after beads clean-up steps. Throughout the course of extensive experimental library optimization, elution volumes were adjusted to accommodate the adapted workflow. Certain samples were included in several different variations for library preparation to allow a direct comparison of the success of different library preparation methods. The final concentrations for the different library preparation methods of single samples can be effectively compared.

The DNA concentration of the final libraries was assessed using the Qubit fluorometer for its accuracy (Table 16). This measurement served both to evaluate the success of library preparation and facilitate precise pooling. Simultaneously, we quantified DNA concentration within the 250-600 bp size range, our target size range, using the TapeStation system. Notably, disparities emerged between these two measurements, primarily due to the recurrent issue of the TapeStation system detecting larger fragments. To enhance clarity, we extended our analysis to include additional size ranges: 25-200 bp, indicating the presence of adapter or primer dimers, and 200-1,500 bp, providing an overview of the remaining DNA fragments. It's important to note that the used DNA Screen Tape for the TapeStation system

is confined to size range measurements between 25 and 1,500 bp. High differences in TapeStation and Qubit measurements might result from fragments larger than 1,500 bp.

Comparing the results of the two methods, G-tailed and non-G-tailed, for samples 12212, 12234, and 16057, it's clear that G-tailing generally leads to higher library concentrations in the 250-600 bp range (Table 16). This trend holds for the overall library concentration as well, except for sample 16057. In this case, the library without G-tailing has a higher overall concentration, likely due to a significant portion of DNA fragments being larger than 1,500 bp.

When contrasting samples subjected to repair with those without repair, it's evident that for sample 13125, the total library concentration was higher in the absence of repair (Table 16). However, the concentration within the 250-600 bp region was greater when the repair approach was applied. For sample 13133, only the repair approach resulted in any detectable concentration.

When contrasting the effects of two different library preparation kits, along with the preceding repair step, on sample 15059, it's evident that the Ultra II kit yielded notably higher DNA concentrations within the 250-600 bp size range than the FS kit (Table 16).

Table 16: Museum Specimen Library Preparation Overview of Samples

Codes: 'x' indicates employed library preparation methods. DNA and dsDNA concentration measurements were taken from DNA extracts using the Qubit Fluorometer. Final Library Concentration of dsDNA was measured using the Qubit Fluorometer. Library Concentration of dsDNA within the 25-200 bp range, 200-1,500 bp range, and 250-600 bp range were assessed using the TapeStation System. Excluded samples are marked with an asterisk (*). Samples with COI sequences are indicated in bold.

ID	DNA (ng/ µl)	dsDNA (ng/ µl)	FFPE-Repair	G-Tailing	Kit	Library (ng/ µl)	25-200 bp (ng/ul)	250-600 bp (ng/ µl)	200-1500 bp (ng/ul)

12196	0.98	too low	x	x	FS	2.12	0.56	0.0895	0.176
12212	4.38	0.824	x		Ultra II	3.30	1.1	0.123	0.235
12212	4.38	0.824	x	x	Ultra II	3.74	1.88	0.352	0.648
12234	13.5	NA	x		Ultra II	too low	0.302	0.154	0.248
12234	13.5	NA	x	x	Ultra II	17.30	4.860	0.864	1.5
12422	11.2	0.75	x	x	FS	8.32	0.268	2.880	3.71
12786	2.92	too low	x	x	FS	15.40	0.915	0.439	0.755
13125	4.2	1.14	x		FS	7.64	0.0259	0.234	0.413
13125	4.2	1.14			FS	15.70	0.698	0.112	0.978
13133	2.3	0.6	x		FS	12.40	0.504	0.0751	0.426
13133*	2.3	1.14			FS	too low	NA	NA	NA
13863	11.1	0.266	x	x	FS	2.60	0.373	0.141	0.218
13917	3.5	0.15	x	x	FS	2.60	0.423	0.0797	0.153
13945*	1.29	7.74	x	x	Ultra II	too low	NA	NA	NA
14102	9.78	2.78	x	x	Ultra II	24.60		0.592	
14367	2.68	too low	x	x	FS	2.48	1.07	0.208	0.374
14401	2.9	0.206	x	x	FS	15.60	1.39	1.18	1.81
14958	16.4	0.62	x	x	FS	4.06	1.51	0.361	0.611
15059	27.2	2.08	x		Ultra II	6.96	1.47	0.599	0.773
15059	**27.2**	**2.08**	**x**	**x**	**FS**	**3.94**	**0.626**	**0.319**	**0.477**
15059	**27.2**	**2.08**	**x**		**FS**	**10.80**	**0.434**	**0.0936**	**0.298**
15504	10.6	0.264	x	x	FS	2.66	0.195	0.459	0.621
15511	5.44	0.472	x	x	Ultra II	32.60	6.85	0.663	1.26
15811	6.76	0.502	x	x	Ultra II	26.80	2.75	0.103	0.865
16057	8.6	NA	x		Ultra II	22.80	0.338	0.102	0.516
16057	8.6	NA	x	x	Ultra II	15.70	5.21	1.020	1.76
16299	24.6	2.76	x	x	FS	15.30	1.530	0.261	0.976
16383	15.6	0.936	x	x	FS	6.78	0.114	1.660	2.250
16964	1.95	too low	x	x	FS	3.44	1.460	0.386	0.7
17346	10.3	0.23	x	x	FS	3.76	1.72	0.383	0.698
17604	**4.54**	**0.345**	**x**	**x**	**FS**	**6.84**	**0.586**	**2.970**	**4.25**
17628	1.51	too low	x	x	FS	3.76	1.380	0.464	0.827
22134*	0.94	too low	x	x	FS	too low	NA	NA	NA
8841*	1.07	too low	x	x	FS	too low	NA	NA	NA
9611	15.1	0.57	x	x	FS	5.34	1.03	0.362	0.639
9682	**59.6**	**3.62**	**x**	**x**	**FS**	**16.40**	**0.137**	**0.197**	**0.711**
9711	3.46	too low	x	x	FS	12.30	NA	NA	NA

Discussion

1. DNA Barcoding and Genetic Diversity

In this study, a total of 317 Isopoda sequences were analyzed, resulting in COI barcode sequences from 29 out of the 64 Austrian Oniscidea species, in addition to sequences from *Asellus aquaticus* (Asellota), totaling 30 identified species. It's important to note that species identification relied on a combination of morphological and molecular methods. Of these 30 putative species, two sequences within the Trichoniscidae family, 26666, and 27243, could not be assigned to a specific species, though they differed from each other and all other Trichoniscidae species. Similarly, we encountered challenges identifying two putative species, one sequence from *Trichoniscus (26603)* and two from *Armadillidium* (27210, 27211) genera. In the case of *Ligidium* cf. *germanicum*, despite its morphological resemblance to *L. germanicum*, a genetic distance of 20% was observed between the two putative species. This genetic differentiation is further supported by Bayesian and species delimitation analyses. Notably, in Genbank, a 3% hit with a single sequence from *L. hypnorum* was found, which is probably an incorrect identification, along with hits of 10-15% with *L. germanicum*. Considering that Austria is known to harbor only *L. germanicum* and *L. hypnorum*, this genetic distinction strongly indicates the potential discovery of a new *Ligidium* species within Austria. This discovery could be attributed to a recent introduction to Austria, or it represents a previously unknown species in the field of science.

The majority of the species not included here belong to the Trichoniscidae family. In my dataset, I have records for only three out of the 25 known Austrian species in this family. The German name for Trichoniscidae is 'Zwergasseln', which translates to 'dwarf woodlice,' underscoring their small size and, consequently, the challenges associated with finding and identifying them. Within Trichoniscidae, there are several species that are endemic or subendemic to Austria, and therefore extremely localized in their distribution (summarized by Allspach 2009). These include *Trichoniscus crassipes, T. karawankianus, T. scheerpeltzi, T.*

steinboecki, T. styricus, and *Haplophthalmus austriacus*, making them challenging to collect and study. Furthermore, there are other (sub)endemic species like *Oroniscus mandli*, known from only one subalpine locality on the Carinthian border with Slovenia (Allspach 2009). Similarly, *Armadillidium carynthiacum* is known from just two submontane localities. Some species have a somewhat larger distribution area outside of Austria, but occur only in a few localities within our country. Among these, we were able to generate a sequence for *Protracheoniscus franzi* using museum material. This species primarily occurs in eastern federal states but is more commonly found in Slovenia, Hungary, and the Czech Republic (Allspach 2009).

Concerning the oniscidean phylogeny, COI data alone may not be sufficient for a comprehensive phylogenetic analysis of Oniscidea. Nevertheless, I will highlight some key aspects. Comparing our findings to previous studies proves challenging. Molecular studies have yielded results distinct from both morphological studies and other molecular investigations, sparking an ongoing debate (Dimitriour et al. 2019, Schmallfuss 2003, Tabacaru & Giurginca 2021). This discours extends to questioning monophyly of Oniscidea within the isopod order, even though strongly supported by morphological synapomorphies (Dimitriou et al. 2019, Schmidt 2008, Tabacaru & Giurginca 2021). Zhang et al. (2019) conducted an extensive examination of Isopoda phylogeny, exploring various datasets including mitochondrial, nuclear, nucleotides, amino acids, concatenated genes, individual genes, and gene orders, employing different phylogenetic algorithms and partitioning strategies. Their findings revealed that nearly all of these approaches yielded different topologies.

Within the Oniscidea order, there are five recognized principal lineages - Ligiidae, Tylidae, Mesoniscidae, Synocheta, Crinocheta (Schmidt 2008). Among these lineages my dataset harbors families belonging to Ligiidae, Crinochaeta (including Agnaridae, Armadillidiidae, Cylisticidae, Oniscidae, Philosciidae, Platyarthridae, Porcellionides, and Trachelipodidae), and Synochaeta (including Trichoniscidae). While these lineages are currently considered

monophyletic, there are some limitations, particularly with regard to Ligiidae (Schmidt 2008). Notably, Ligiidae, comprising solely *Ligidium*, forms a well supported monophyletic group. In a prior study from Mattern and Schlegel (2001), they delved into the phylogenetics of primarily German oniscidean species using multiple approaches such as neighbor-joining (NJ), maximum-parsimony (MP), and maximum-likelihood (ML) with the small subunit ribosomal DNA (ssu rDNA). Their outcomes revealed varying relationships within each oniscidean lineage, contingent on the phylogenetic technique utilized. Nevertheless, it's noteworthy that these lineages consistently yielded monophyletic taxa. Conversely, Crinochaeta and Synochaeta are not monophyletic in my dataset. Notably, *Platyarthrus hoffmannseggii* and *Asellus aquaticus* classified within the Synochaeta. Also, sequence 28422 from Trichniscidae is included within the Crinochaeta group. However, the backbone of my Bayesian tree remains unresolved. This could potentially be attributed to the inadvertent inclusion of sequences from *Daphnia, Gammarus,* and *Asellus*. This raises the question whether running the Bayesian phylogenetic analysis again without these non-oniscidean sequences might yield a different topology.

An argument supporting the presence of cryptic species within my dataset emerges by comparing the number of morphospecies to the species delineation analyses. While morphological identifications, including *Asellus aquaticus*, identified 30 isopod species, species delineation analysis suggest a minimum of 35 putative species (ASAP1) and a maximum of 52 putative species (GMYC). This disparity underscores the potential existence of hidden species diversity within these species. Notably, there are high intraspecific genetic distances in several species including *Armadillidium versicolor* (5.4%), *Armadillidium vulgare* (6.5%), *Cylisticus convexus* (6.3%), *Porcellio scaber* (5.8%), *Porcellium collicola* (13.9%), *Trachelipus rathkii* (5.4%), *Trachelipus ratzeburgii* (10.4%), and *Tracheoniscus pusillus* (11.7%). This aligns with Raupach et al. (2022), who also identified considerable genetic divergence within several isopod species, with some overlapping with our results. For instance, they observed an intraspecific genetic divergence of 6.44% in *Armadillidium*

vulgare, 12.16% in *Porcellio scaber*, 16.59% in *Trachelipus rathkii*, and 13.47% in *Tracheoniscus pusillus*. The genetic differentiation observed in European woodlice species, as measured by COI and other mitochondrial markers, may be influenced by various factors, as summarized by Raupach et al. (2022).

These factors include the species' geographic history, encompassing events such as migrations, regional isolation, and adaptations to varying environments (Bedek et al. 2019, Klossa-Kilia et al. 2005, Raupach et al. 2014). It's important to note that our dataset has geographic gaps, and therefore, we cannot discount the potential influence of isolation by distance on the observed genetic patterns. This becomes particularly evident in the case of *Porcellium collicola,* where two distinct lineages emerge. One lineage is composed of individuals exclusively from Vienna, while the other forms a distinct clade found in Styria and Carinthia. While this geographical segregation within a single putative species suggests that restricted mobility and regional isolation could contribute to intraspecific divergence, additional sampling in intermediate regions is necessary to provide a comprehensive understanding of the genetic structure. For the majority of the species, which were collected across a wide geographic range in Austria, such an observation of clustering of haplotypes by sampling sites was not made. For instance, *Lepidoniscus minutus* was collected in Vienna, Styria, Carinthia, and Lower Austria, yet it exhibited only a modest intraspecific divergence of 1.4%. *Armadillidium vulgare* was subdivided into three major clades: *A. vulgare* A, *A. vulgare* B, and *A. vulgare* C-E. Each of these clades exhibited a wide range of sampling sites across several federal states, often overlapping with one another in sympatry. Furthermore, the presence of the inherited alpha-proteobacteria *Wolbachia* Hertig, 1936, has been shown to induce extensive intraspecific variation to the extent that a single species may appear as two distinct species (Hurst & Jiggins 2005). This bacterium infects numerous isopod species, including Oniscidea, and significantly alters the biology of their hosts, such as by feminization, parthenogenesis, male killing, and sperm-egg incompatibility (Bouchon et al. 2008, Cordaux & Gilbert 2017, Delhoumi et al. 2019). Moreover, another intriguing phenomenon is observed in *Armadillidium vulgare*, where certain populations lacking

Wolbachia exhibit a unique pattern of feminization (Cordaux & Gilbert 2017, Leclerq et al. 2016). In these populations, feminization of genetic males through an enigmatic factor termed the 'f element' occurs (Cordaux & Gilbert 2017, Leclerq et al. 2016). This 'f element' is an instance of recent horizontal transfer induced by *Wolbachia* (Cordaux & Gilbert 2017, Leclerq et al. 2016).

Additionally, the accurate assessment of mitochondrial variability within a species can be hindered by the amplification of nuclear mitochondrial pseudogenes (numts) (Buhay 2009). While 'COI-like' numts have not been reported in isopods to date, they have been documented in various crustacean taxa, with some available in the Genbank database (Buhay 2009, Kim et al. 2013). Given the effort to establish universal primers for COI, suitable to almost all animal taxa, there's a possibility that in some taxa these primers have a higher affinity to the nuclear copies of COI. This can result in the amplification and sequencing of numts rather than the authentic mitochondrial sequence. Consequently, leading to artificially high sequence divergences within a species and giving the false impression of the presence of cryptic species. However, there is no indication of the presence of numts in my dataset, as there are no stop codons or frameshift mutations.

Finally, it's worth noting that several oniscid species have been reported to possess distinctive mitochondrial DNA structures. These structures involve both linear monomers and circular dimers, formed by merging two mitochondrial genome copies together in a palindrome-like arrangement (Pearman 2022). This unique configuration gives rise to distinct mitochondrial lineages within a species (Doublet et al. 2013, Pearman et al. 2022) and may also be linked to heteroplasmy, where multiple mtDNA genotypes coexist within an organism (Chandler et al. 2015, Doublet et al. 2013). It’s important to note that, based on our dataset, there are no clear indications of heteroplasmy. The two copies of the circular genome can exhibit dissimilarities in certain isopod species, as shown by single nucleotide polymorphisms (SNPs) (Chandler et al. 2015, Pearman 2022). Nevertheless, in-depth research in this domain remains limited, leaving the implications of these unusual mitochondrial structures on DNA barcoding uncertain.

Several studies have observed significant genetic diversity within terrestrial isopod species, with some suggesting the presence of potentially cryptic species (Bedek et al. 2019, Eberl et al. 2013, Klossa-Kilia et al. 2005, Raupach et al. 2022). Parmakelis (2008) documented a genetic distance of 13.9% and 14.2% between different populations of *Trachelipus kytherensis*. Delhoumi et al. (2019) discovered genetic distances exceeding 35% in 16S rRNAamong various populations of *Porcellionides pruinosus* in Tunisia. For marine Isopoda privious studies suggest that intraspecific COI distances are typically below 6%, with some instances reaching up to 8%, while interspecific distances usually exceed 10% (Bober et al. 2019, Brix et al. 2014, Paulus et al. 2022). This pattern aligns most closely with the ASAP partition denoted by the highest ASAP score, ASAP1, which sets a threshold distance of 12%. Consequently, it suggests that *Porcellium collicola*, *Trachelipus ratzeburgii*, and *Tracheoniscus pusillus* may encompass more than one species. The presence of two divergent lineages separated by up to 13.9% in *Porcellium collicola* might be attributed to geographical isolation within a single species, as mentioned above, although more extensive sampling is required to confirm this hypothesis. *Trachelipus ratzeburgii* A and *T. ratzeburgii* B-C were collected from overlapping federal states, and Bayesian phylogenetic analysis provides robust posterior probabilities for each clade. These observations collectively suggest the possibility of cryptic species within the *T. ratzeburgii* lineage. Finally, in the case of *Trichoniscus pusillus*, our dataset consists of only two sequences from markedly distant sampling sites in Tirol and Lower Austria. Both sequences were assigned to *T. pusillus* based on matches in Genbank and BOLD database, however, they were assigned to different Barcode Index Numbers (BINs). Morphological identification was challenging because both individuals were female, and precise species-level identification, typically for isopods, relies on male characteristics. While it's probable that they are indeed *T. pusillus*, this can only be confirmed with certainty by obtaining data from male specimens. The question of whether these lineages represent cryptic species or if their genetic divergence is

primarily a result of geographic separation remains open and necessitates further data collection, specifically targeting male individuals.
Additionally, it's important to emphasize that species with small sample sizes and limited geographic coverage, such as *Haplothalmus danicus, Ligidium* cf. *germanicum, Ligidium hypnorum, Platyarthrus hoffmannseggii, Asellus aquaticus, Oniscus asellus, Philoscia muscorum*, and *Porcellionides pruinosus,* may lead to an underestimation of diversity. This incomplete sampling may not capture all existing genetic variations and distinct lineages within these species, potentially leading to an underestimation of overall biodiversity in the study area.

While DNA barcoding is indeed a powerful tool for identifying known species and detecting previously undiscovered ones, it is vital to remember that taxonomic conclusions should be drawn by integrating various forms of data, including nuclear markers and morphological identifications (Bober et. al 2019, Brower 2010, Meier et al. 2006, Schlick-Steiner et al. 2010, Tan et al. 2010, Will et al. 2005). Notably, although significant genetic differences can uncover cryptic taxa, an exclusive reliance on DNA barcoding may risk prematurely defining species boundaries and overlooking other factors influencing genetic variation within a species.

In conclusion, this study highlights significant genetic diversity within Austrian Isopoda. Notably, providing evidence suggesting the presence of a new *Ligidium* species in Austria and proposing the existence of cryptic species within *Trachelipus ratzeburgii.* Additionally, there are indications of potential cryptic diversity within *Porcellium collicola* and *Trichoniscus pusillus*, however, further data collection is required to confirm these hypotheses. Factors like geographic history, limited dispersal capabilities, the influence of *Wolbachia*, and unique mitochondrial DNA structures may contribute to intraspecific divergence. These factors underscore the complexity of species delineation in isopods and emphasize the importance of comprehensive genetic analysis for a deeper understanding of their evolutionary history.

To achieve precise taxonomy inference, it is recommended to incorporate a range of data sources such as nuclear markers and morphology-based identifications. While DNA barcoding is a robust tool for species identification, it is important to utilize additional methods to gain a comprehensive understanding of genetic variation within species.

2. DNA Barcoding of Historic Specimen

My research demonstrates the success and feasibility of amplifying mini-barcodes from historical isopod specimens using Sanger sequencing when compared to Illumina sequencing. Sanger sequencing yielded a significantly higher success rate, generating a total of 15 sequences from various specimens, while Illumina sequencing provided only four COI sequences, representing three different species. Importantly, Sanger sequencing not only outperformed Illumina in terms of success but also proved to be a more cost-effective and efficient method in this study.

The 15 historical mini-barcodes correspond to a success rate of 18.75%. Comparing my results to previous studies, mini-barcodes have proven to be a valuable tool for the identification of historical specimens. Meusnier et al. (2008) achieved a 100% success rate in generating mini-barcodes from dried Coleophora specimens dating back to 1871-1944. It's worth noting that their success was likely influenced by working with dried specimens, which typically exhibit less DNA degradation compared to other preservation methods. Baird et al. (2011) encountered challenges when attempting to obtain full-length COI barcodes from caddisfly specimens with varying ages, reporting a success rate of only 2.9%. However, when employing mini-barcodes, their success rate notably improved to 17.5%. Similarly, Hajibabaei et al. (2006) worked with wasps, which were either dried or preserved in ethanol. These specimens were collected in Costa Rica and ranging from 1 to 14 years old. While their success rate for full-length barcodes was 24%, they achieved higher success rates of 84% and 98% when recovering two different mini-barcodes. These collective findings affirm

the value of mini-barcodes not only for confidently identifying historical specimens but also for generating barcodes for species that might otherwise be poorly represented in barcode databases. This is supported by the absence of substantial differences observed when compared to full-length COI barcodes. This is also supported by my dataset. Historical sequences obtained using mini-barcodes either cluster with their corresponding putative species with 100% similarity to other sequences, or, in cases where only a single sequence per species is present, they form distinct clusters. These results underscore the efficacy of mini-barcodes as a robust alternative for identifying historical specimens characterized by degraded DNA, presenting a potent asset for biodiversity research and species identification. The efficacy of the previous FFPE repair step in mini-barcode generation becomes apparent when considering the experimental PCR results. In this analysis, 33.3% (seven out of 21 samples) successfully generated mini-barcodes when utilizing the FFPE repair step, as opposed to a lower success rate of 19% (four out of 21 samples) without FFPE repair. Only in sample 17346, a dual signal for both ‘C’ and ‘T’ at a single nucleotide position was detected in both the repaired and unrepaired sequences. Hence, the higher success rate is likely attributed to the repair of crosslinks and single-strand breaks rather than deamination repair.

Next-Generation Sequencing (NGS) is commonly used for processing historical samples due to its potential advantages over Sanger sequencing, such as reduced amplification bias, and the ability to work with fragmented DNA templates (Prosser et al. 2016). Previous studies have shown promising results with NGS (Hoban et al. 2022, Prosser et al. 2016). However, in my study, NGS performed poorly. This might be partly due to technical difficulties with the TapeStation system, which led to pooling libraries based on inaccurate concentration measurements. This issue likely resulted in insufficient coverage for the assembly and recovery of the COI sequences.

As a result, a high variation in the number of reads per library was observed, leading to over- or underrepresentation of certain samples. This likely resulted in insufficient coverage for the

assembly and recovery of the COI sequences. Additionally, a substantial proportion of reads seemed to be associated with primer or adapter sequences, indicating the presence of a notable amount of primer dimers or polymers within our libraries. To address this issue, it may be advisable to reduce the concentrations of adapters used during the library preparation process.

A protocol for preparing libraries from historical specimens for Illumina Sequencing was developed. This protocol includes a repair step using BioLabs' NEBNext FFPE DNA Repair v2 Module to address FFPE-induced damage. Additionally, I employ a G-tailing and C-Primer ligation step to convert ssDNA to dsDNA, optimizing DNA yield with precise reagent ratios. For sequencing, I chose between two NEB kits: the NEBNext Ultra II DNA Library Prep Kit and, for additional fragmentation needs, the NEBNext Ultra II FS DNA Library Prep Kit. All four Illumina COI barcode sequences were generated using the FS Kit. Because the study doesn't follow a fully factorial approach, I can't directly compare the kits or library preparation methods. Furthermore, due to the poor success rate of COI data from NGS, it's not possible to definitively determine which steps are crucial. However, estimating the importance of certain steps can be done by comparing DNA concentrations in libraries. Notably, the repair step increased the amount of amplified DNA for the 250-600 bp region in two samples where libraries with and without FFPE repair could be compared. Given the favorable outcomes of the repair step prior to mini-barcode amplification (see above), it appears to be a valuable addition to the protocol. For G-tailing, the three samples that are comparable also exhibit higher concentrations in the 250-600 bp range. However, considering that this step is quite time-consuming, I would suggest conducting further tests to validate its significance. In the case of the single sample where both library preparation kits were compared, Ultra II notably yielded a higher DNA concentration in the 250-600 bp range. It's important to note that these comparisons rely on Tapestation measurements, which should be interpreted with caution. Further conclusions can be drawn after a more exhaustive analysis of the data.

In summary, the study of historical isopod specimens has presented a unique challenge due to their limited DNA content, compounded by the small size of these organisms. Despite these inherent challenges, the acquisition of sequences from museum specimens, each representing a different species of Oniscidea, has proven to be of exceptional value. These mini-barcodes from historical samples, accompanied by taxonomic identifications from experts, fill critical gaps in COI databases. They are particularly valuable for species that are rare, challenging to collect, or possess limited representation in the Genbank database. Hence, they hold immense promise for DNA barcoding studies and initiatives like ABOL, enabling us to broaden our understanding of isopod taxonomy and diversity. While this study focused on generating barcodes from 80 unique specimens, it underscores the potential of a more targeted approach, involving multiple specimens, for future research dedicated to specific species.

References

- Allio, R., Schomaker‐Bastos, A., Romiguier, J., Prosdocimi, F., Nabholz, B., & Delsuc, F. (2020). MitoFinder: Efficient automated large‐scale extraction of mitogenomic data in target enrichment phylogenomics. *Molecular Ecology Resources*, *20*(4), 892-905.
- Allspach, A. (2009). Terrestrische Crustacea (Landasseln). *endemiten-kostbarkeiten in Österreichs Pflanzen-und Tierwelt,* 398-404
- Baird, D. J., Pascoe, T. J., Zhou, X., & Hajibabaei, M. (2011). Building freshwater macroinvertebrate DNA-barcode libraries from reference collection material: formalin preservation vs specimen age. *Journal of the North American Benthological Society*, *30*(1), 125-130.
- Bedek, J., Taiti, S., Bilandžija, H., Ristori, E., & Baratti, M. (2019). Molecular and taxonomic analyses in troglobiotic Alpioniscus (Illyrionethes) species from the Dinaric Karst (Isopoda: Trichoniscidae). *Zoological Journal of the Linnean Society*, *187*(3), 539-584.
- Bober, J., Brandt, A., Frutos, I., & Schwentner, M. (2019). Diversity and distribution of ischnomesidae (Crustacea: Isopoda: Asellota) along the Kuril-Kamchatka Trench–a genetic perspective. *Progress in Oceanography*, *178*, 102174.
- Bouchon, D., Cordaux, R., & Grève, P. (2008). Feminizing Wolbachia and the evolution of sex determination in isopods. *Insect symbiosis*, *3*, 273-294.
- Bouckaert, R., Vaughan, T. G., Barido-Sottani, J., Duchêne, S., Fourment, M., Gavryushkina, A., ... & Drummond, A. J. (2019). BEAST 2.5: An advanced software platform for Bayesian evolutionary analysis. *PLoS computational biology*, *15*(4), e1006650.
- Boyko, C. B., Bruce, N. L., Hadfield, K. A., Merrin, K. L., Ota, Y., Poore, G. C. B., Taiti, S. (Eds) (2008 onwards). World marine, freshwater and terrestrial isopod crustaceans database. Accessed at https://www.marinespecies.org/isopoda on 2023-03-08.
- Brix, S., Svavarsson, J., & Leese, F. (2014). A multi-gene analysis reveals multiple highly divergent lineages of the isopod Chelator insignis (Hansen, 1916) south of Iceland. *Polish Polar Research*, 225-242.

- Brower, A. V. (2010). Alleviating the taxonomic impediment of DNA barcoding and setting a bad precedent: names for ten species of ‘Astraptes fulgerator’(Lepidoptera: Hesperiidae: Eudaminae) with DNA-based diagnoses. *Systematics and Biodiversity*, *8*(4), 485-491.
- Buhay, J. E. (2009). “COI-like” sequences are becoming problematic in molecular systematic and DNA barcoding studies. *Journal of crustacean biology*, *29*(1), 96-110.
- Chandler, C. H., Badawi, M., Moumen, B., Grève, P., & Cordaux, R. (2015). Multiple conserved heteroplasmic sites in tRNA genes in the mitochondrial genomes of terrestrial isopods (Oniscidea). *G3: Genes, Genomes, Genetics*, *5*(7), 1317-1322.
- Cordaux, R., & Gilbert, C. (2017). Evolutionary significance of Wolbachia-to-animal horizontal gene transfer: female sex determination and the f element in the isopod Armadillidium vulgare. *Genes*, *8*(7), 186.
- Delhoumi, M., Zaabar, W., Bouslama, M. F., Zayani, D., & Achouri, M. S. (2019). High level of genetic variation in mitochondrial 16S rDNA among populations of Porcellionides pruinosus (Brandt, 1833)(Crustacea: Isopoda: Oniscidea) in Tunisia. *The European Zoological Journal*, *86*(1), 1-8.
- Dimitriou, A. C., Taiti, S., & Sfenthourakis, S. (2019). Genetic evidence against monophyly of Oniscidea implies a need to revise scenarios for the origin of terrestrial isopods. *Scientific reports*, *9*(1), 18508.
- Do, H., & Dobrovic, A. (2015). Sequence artifacts in DNA from formalin-fixed tissues: causes and strategies for minimization. *Clinical chemistry*, *61*(1), 64-71.
- Doublet, V., Helleu, Q., Raimond, R., Souty-Grosset, C., & Marcadé, I. (2013). Inverted repeats and genome architecture conversions of terrestrial isopods mitochondrial DNA. *Journal of molecular evolution*, *77*, 107-118.
- Eberl, R., Mateos, M., Grosberg, R. K., Santamaria, C. A., & Hurtado, L. A. (2013). Phylogeography of the supralittoral isopod L igia occidentalis around the Point Conception marine biogeographical boundary. *Journal of Biogeography*, *40*(12), 2361-2372.
- Elbrecht, V., & Leese, F. (2017). Validation and development of COI metabarcoding primers for freshwater macroinvertebrate bioassessment. *Frontiers in Environmental Science*, *5*, 11.

- Folmer, O., Black, M., Hoeh, W., Lutz, R., & Vrijenhoek, A. R. (1994). DNA primers for amplification of mitochondrial cytochrome c oxidase subunit I from diverse metazoan invertebrates. Mol. Mar. Biol. Biotechnol.
- Hajibabaei, M., Smith, M. A., Janzen, D. H., Rodriguez, J. J., Whitfield, J. B., & Hebert, P. D. (2006). A minimalist barcode can identify a specimen whose DNA is degraded. *Molecular Ecology Notes*, *6*(4), 959-964.
- Hebert, P. D., Cywinska, A., Ball, S. L., & DeWaard, J. R. (2003). Biological identifications through DNA barcodes. *Proceedings of the Royal Society of London. Series B: Biological Sciences*, *270*(1512), 313-321.
- Hebert, P. D., Penton, E. H., Burns, J. M., Janzen, D. H., & Hallwachs, W. (2004). Ten species in one: DNA barcoding reveals cryptic species in the neotropical skipper butterfly Astraptes fulgerator. *Proceedings of the National Academy of Sciences*, *101*(41), 14812-14817.
- Hoban, M. L., Whitney, J., Collins, A. G., Meyer, C., Murphy, K. R., Reft, A. J., & Bemis, K. E. (2022). Skimming for barcodes: rapid production of mitochondrial genome and nuclear ribosomal repeat reference markers through shallow shotgun sequencing. *PeerJ*, *10*, e13790.
- Hurst, G. D., & Jiggins, F. M. (2005). Problems with mitochondrial DNA as a marker in population, phylogeographic and phylogenetic studies: the effects of inherited symbionts. *Proceedings of the Royal Society B: Biological Sciences*, *272*(1572), 1525-1534.
- Kim, S. J., Lee, K. Y., & Ju, S. J. (2013). Nuclear mitochondrial pseudogenes in Austinograea alayseae hydrothermal vent crabs (Crustacea: Bythograeidae): effects on DNA barcoding. *Molecular ecology resources*, *13*(5), 781-787.
- Klossa-Kilia, E., Kilias, G., & Sfenthourakis, S. (2005). Increased genetic diversity in Greek populations of the genus Ligidium (Crustacea: Isopoda: Oniscidea) revealed by RFLP analysis of mtDNA segments. *Contributions to Zoology*, *74*(3-4), 255-264.
- Kress, W. J., & Erickson, D. L. (2012). *DNA barcodes: methods and protocols* (pp. 3-8). Humana Press.
- Leclercq, S., Thézé, J., Chebbi, M. A., Giraud, I., Moumen, B., Ernenwein, L., ... & Cordaux, R. (2016). Birth of a W sex chromosome by horizontal transfer of Wolbachia bacterial symbiont genome. *Proceedings of the National Academy of Sciences*, *113*(52), 15036-15041.

- Mattern, D., & Schlegel, M. (2001). Molecular evolution of the small subunit ribosomal DNA in woodlice (Crustacea, Isopoda, Oniscidea) and implications for Oniscidean phylogeny. *Molecular Phylogenetics and Evolution*, *18*(1), 54-65.
- Matzen da Silva, J., Creer, S., Dos Santos, A., Costa, A. C., Cunha, M. R., Costa, F. O., & Carvalho, G. R. (2011). Systematic and evolutionary insights derived from mtDNA COI barcode diversity in the Decapoda (Crustacea: Malacostraca). *PLoS one*, *6*(5), e19449.
- Meier, R., Shiyang, K., Vaidya, G., & Ng, P. K. (2006). DNA barcoding and taxonomy in Diptera: a tale of high intraspecific variability and low identification success. *Systematic biology*, *55*(5), 715-728.
- Meyer, C. P., & Paulay, G. (2005). DNA barcoding: error rates based on comprehensive sampling. *PLoS biology*, *3*(12), e422.
- Meusnier, I., Singer, G. A., Landry, J. F., Hickey, D. A., Hebert, P. D., & Hajibabaei, M. (2008). A universal DNA mini-barcode for biodiversity analysis. *BMC genomics*, *9*(1), 1-4.
- Parmakelis, A., Klossa-Kilia, E., Kilias, G., Triantis, K. A., & Sfenthourakis, S. (2008). Increased molecular divergence of two endemic Trachelipus (Isopoda, Oniscidea) species from Greece reveals patterns not congruent with current taxonomy. *Biological Journal of the Linnean Society*, *95*(2), 361-370.
- Paulus, E., Brix, S., Siebert, A., Martinez Arbizu, P., Rossel, S., Peters, J., ... & Schwentner, M. (2022). Recent speciation and hybridization in Icelandic deep‐sea isopods: An integrative approach using genomics and proteomics. *Molecular Ecology*, *31*(1), 313-330.
- Pearman, W. S., Wells, S. J., Dale, J., Silander, O. K., & Freed, N. E. (2022). Long-read sequencing reveals atypical mitochondrial genome structure in a New Zealand marine isopod. *Royal Society Open Science*, *9*(1), 211550.
- Prosser, S. W., deWaard, J. R., Miller, S. E., & Hebert, P. D. (2016). DNA barcodes from century‐old type specimens using next‐generation sequencing. *Molecular ecology resources*, *16*(2), 487-497.
- Puillandre, N., Brouillet, S., & Achaz, G. (2021). ASAP: assemble species by automatic partitioning. *Molecular Ecology Resources*, *21*(2), 609-620.

- Rambaut, A., Drummond, A. J., Xie, D., Baele, G., & Suchard, M. A. (2018). Posterior summarization in Bayesian phylogenetics using Tracer 1.7. *Systematic biology*, *67*(5), 901-904.
- Raupach, M. J., Bininda-Emonds, O. R., Knebelsberger, T., Laakmann, S., Pfaender, J., & Leese, F. (2014). Phylogeographical analysis of Ligia oceanica (Crustacea: Isopoda) reveals two deeply divergent mitochondrial lineages. *Biological Journal of the Linnean Society*, *112*(1), 16-30.
- Raupach, M. J., Rulik, B., & Spelda, J. (2022). Surprisingly high genetic divergence of the mitochondrial DNA barcode fragment (COI) within Central European woodlice species (Crustacea, Isopoda, Oniscidea). *ZooKeys*, *1082*, 103.
- Schlick-Steiner, B. C., Steiner, F. M., Seifert, B., Stauffer, C., Christian, E., & Crozier, R. H. (2010). Integrative taxonomy: a multisource approach to exploring biodiversity. *Annual review of entomology*, *55*, 421-438.
- Schmalfuss, H. (2003). World catalog of terrestrial isopods (Isopoda: Oniscidea). [Updated by Schmalfuss in 2004]
- Schmidt, C. (2008). Phylogeny of the terrestrial Isopoda (Oniscidea): a review. *Arthropod systematics & phylogeny*, *66*, 191-226.
- Schmölzer, K. (1965). Ordnung Isopoda (Landasseln).
- Sonnenberg, R., Nolte, A. W., & Tautz, D. (2007). An evaluation of LSU rDNA D1-D2 sequences for their use in species identification. *Frontiers in zoology*, *4*(1), 1-12.
- Strouhal, H. (1951). *Die österreichischen Landisopoden, ihre Herkunft und ihre Beziehungen zu den Nachbarländern*. Zoologisch-Botanische Ges..
- Tabacaru, I., & Giurginca, A. (2021). The Monophyly and the Classification of the Terrestrial Isopods (Crustacea, Isopoda, Oniscidea). *Trav. Inst. Speol. Emile Racovitza*, *59*, 3-23.
- Tamura, K., Stecher, G., & MEGA11, S. K. Molecular Evolutionary Genetics Analysis Version 11., 2021, 38. *DOI: https://doi. org/10.1093/molbev/msab120*, 3022-3027.
- Tan, D. S., Ang, Y., Lim, G. S., Ismail, M. R. B., & Meier, R. (2010). From ‘cryptic species’ to integrative taxonomy: an iterative process involving DNA sequences, morphology, and behaviour leads to the resurrection of Sepsis pyrrhosoma (Sepsidae: Diptera). *Zoologica Scripta*, *39*(1), 51-61.

- Tin, M. M. Y., Economo, E. P., & Mikheyev, A. S. (2014). Sequencing degraded DNA from non-destructively sampled museum specimens for RAD-tagging and low-coverage shotgun phylogenetics. *PloS one*, *9*(5), e96793.
- Wagstaff, S. J., & Garnock‐Jones, P. J. (1998). Evolution and biogeography of the Hebe complex (Scrophulariaceae) inferred from ITS sequences. *New Zealand Journal of Botany*, *36*(3), 425-437.
- White, T. J., Bruns, T., Lee, S. J. W. T., & Taylor, J. (1990). Amplification and direct sequencing of fungal ribosomal RNA genes for phylogenetics. *PCR protocols: a guide to methods and applications*, *18*(1), 315-322.
- Will, K. W., Mishler, B. D., & Wheeler, Q. D. (2005). The perils of DNA barcoding and the need for integrative taxonomy. *Systematic biology*, *54*(5), 844-851.
- Zhang, D., Zou, H., Hua, C. J., Li, W. X., Mahboob, S., Al-Ghanim, K. A., ... & Wang, G. T. (2019). Mitochondrial architecture rearrangements produce asymmetrical nonadaptive mutational pressures that subvert the phylogenetic reconstruction in Isopoda. *Genome biology and evolution*, *11*(7), 1797-1812.

Appendix

Appendix A: List of Museum Specimens and total DNA (ss) and double-strand (ds) Concentrations according to Qubit Measurement.

Codes 'x' indicates employed sequencing methods: Sanger Sequencing or Illumina (NGS). Samples where COI sequences were obtained from Illumina are indicated in bold.

ID	Species	ss (ng/µl)	ds (ng/µl)	Sanger	NGS
8816	*Mesoniscus alpicola alpicola*	0.76	NA		
8841	*Titanethes dahli*	1.07	too low		x
8866	*Trichoniscus austriacus*	0.34	too low		
8929	*Trichoniscus crassipes*	too low	too low		
9092	*Trichoniscus muscivagus*	0.7	too low		
9123	*Trichoniscus elisabethae*	too low	too low		
9151	*Trichoniscus nivatus*	0.58	too low		
9201	*Trichoniscus noricus noricus*	0.54	too low		
9316	*Hyloniscus riparius*	3.94	0.24		
9474	*Trichoniscus ostarrichius*	0.34	too low		
9611	*Tracheoniscus pseudoratzeburgi apenninorum*	15.1	0.57		x
9682	***Hyloniscus riparius***	**59.6**	**3.62**		**x**
9711	*Tracheoniscus pseudoratzeburgi apenninorum*	3.46	too low		x
9742	*Trichoniscus pygmaeus horticola*	too low	too low		
11106	*Hyloniscus riparius*	1.78	too low		
11192	*Haplophthalmus danicus danicus*	too low	NA		
11247	*Haplophthalmus austriacus*	too low	NA		
11292	*Haplophthalmus legrandi*	0.58	too low		
11334	*Haplophthalmus montivagus*	1.4	too low		
11499	*Protracheoniscus politus ab. ubliensis*	too low	0.146		
11519	*Haplophthalmus mariae*	NA	too low		
11529	*Haplophthalmus mengii*	too low	too low		
12184	*Calconiscellus karawankianus*	1.92	0.204		
12196	*Oniscus asellus ab. nodulosus*	0.98	NA		x
12212	*Oniscus asellus var. murarius*	4.38	0.824	x	x
12234	*Oniscus asellus*	13.5	NA		x
12276	*Philoscia germanica*	1.95	0.128		

12355	*Haplophthalmus mengii*	1.92	too low		
12422	*Lepidoniscus minutus pannonicus*	11.2	0.75	**x**	x
12547	*Hyloniscus adonis ab. carniolensis*	0.34	NA		
12786	*Hyloniscus riparius*	2.92	too low		x
12862	*Hyloniscus adonis*	0.82	too low		
13021	*Cylisticus convexus*	0.98	too low		
13124	*Cylisticus convexus*	too low	too low		
13125	*Cylisticus convexus*	4.2	1.14		x
13133	*Cylisticus convexus*	2.3	0.6		x
13740	*Protracheoniscus hermagorensis*	1.52	too low		
13775	*Protracheoniscus franzi*	2.02	2.02	**x**	
13816	*Protracheoniscus amoenus amoenus*	1.09	NA		
13863	*Protracheoniscus politus* ab. *ubliensis*	11.1	0.266	**x**	x
13917	*Trichoniscus pygmaeus horticola*	3.5	0.15		x
13927	*Tracheoniscus rathkei* ab. *trilineatus*	0.28	too low		
13945	*Tracheoniscus rathkei* ab. *trilineatus*	7.74	1.29		x
13947	*Tracheoniscus rathkei* ab. *trilineatus*	0.48	too low		
13965	*Tracheoniscus ratzeburgi*	too low	too low		
14102	*Tracheoniscus rathkei rathkei*	9.78	2.78	**x**	x
14264	*Tracheoniscus balticus balticus*	5.12	NA	**x**	
14339	*Trachelipus rathkei rathkei*	1.18	0.416	**x**	
14367	*Protracheoniscus amoenus amoenus*	2.68	NA		x
14401	*Tracheoniscus pseudoratzeburgi apenninorum*	2.9	0.206		x
14945	*Porcellio laevis*	1.53	0.62		
14958	*Porcellio nodulosus*	16.4	0.62		x
15032	*Porcellio pictus*	1.88	0.408		
15059	***Porcellio pictus***	**27.2**	**2.08**	**x**	**x**
15070	*Porcellio pictus*	too low	too low		
15105	*Porcellio scaber* ab. *scaber*	19	1.08		
15504	*Hyloniscus riparius*	10.6	0.264		
15511	*Porcellio scaber* ab. *marmoratus*	5.44	0.472		x
15804	*Porcellio scaber* ab. *scaber*	8.44	0.534		x
15811	*Porcellio laevis laevis*	6.76	0.502	**x**	x
15893	*Porcellio spinicornis*	0.52	0.1	**x**	
15970	*Porcellio scaber scaber*	1.12	0.332	**x**	
16057	*Porcellium fiumanum fiumanum*	8.6	NA		x
16163	*Porcellium graevei*	6.88	0.15		

16192	*Porcellium collicola*	1.82	too low		
16299	*Porcellium fiumanum salisburgense*	24.6	2.76		x
16383	*Porcellium conspersum*	15.6	0.936	**x**	x
16669	*Porcellio frontalis*	1.68	too low		
16942	*Platyarthrus hoffmannseggi*	0.6	too low		
16964	*Metoponorthus cingendus*	1.95	too low		x
17115	*Porcellio scaber* ab. *scaber*	10.1	0.55		
17119	*Armadillidium verhoeffi*	12	0.848		
17346	*Protracheoniscus politus* ab. *ubliensis*	10.3	0.23	**x**	x
17478	*Armadillidium verhoeffi*	75	6.48		
17581	*Armadillidium verhoeffi*	48.8	4.64		
17604	***Armadillidium carniolense***	**4.54**	**0.354**	**x**	**x**
17628	*Armadillidium carynthiacum*	1.51	NA		x
17679	*Armadillidium nasatum nasatum*	0.6	too low	**x**	
17807	*Armadillidium vulgare* var. *decipiens*	12.4	2.76		
22134	*Protracheoniscus asiaticus*	0.94	NA		x

Appendix B: COI Distance Matrix.

Species listed according to GMYC species delimitation analysis. Distance ranges are displayed in %.

	Ligidium germanicum	*Ligidium hypnorum*	*Ligidium cf. germanicum*	*Ligidium cf. germanicum*	*Platyarthrus hoffmannseggii*	*Haplophthalmus mengii*	*Oniscus asellus*	*Asellus aquaticus*	*Philoscia muscorum*	*Philoscia affinis*	*Haplophtalmus danicus*	*Trichoniscus sp.*	*Trichoniscidae A*	*Hyloniscus riparius*	*Trichoniscidae B*	*Trichoniscus pusillus A*	*Trichoniscus pusillus B*	*Porcellionides pruinosus*	*Porcellio spinicornis*	*Armadillidium pictum*	*Armadillidium vesicolor A*
Ligidium germanicum	0-0,4	-	-	-	-	-	-	-	-	-	-	-	-	-	-	-	-	-	-	-	-
Ligidium hypnorum	20,9-21,4	0-0	-	-	-	-	-	-	-	-	-	-	-	-	-	-	-	-	-	-	-
Ligidium cf. *germanicum*	18,5-19	19-19	0-0	-	-	-	-	-	-	-	-	-	-	-	-	-	-	-	-	-	-
Ligidium cf. *germanicum*	19,3-20	18-18,5	3,6-3,8	0-0,2	-	-	-	-	-	-	-	-	-	-	-	-	-	-	-	-	-
Platyarthrus hoffmannseg	34,8-35,1	30,9-31	31,7-32	31,7-33	0-0	-	-	-	-	-	-	-	-	-	-	-	-	-	-	-	-
Haplophthalmus mengii	29,3-29,7	29-29	30,4-30,4	30,8-31,2	28,4-28,7	0-0	-	-	-	-	-	-	-	-	-	-	-	-	-	-	-
Oniscus asellus	30,8-31,5	27,7-28,7	30,3-31,8	30,3-31,2	27,9-29,5	26,5-28,6	0-4,1	-	-	-	-	-	-	-	-	-	-	-	-	-	-
Asellus aquaticus	28,1-29,2	29,2-29,2	29,3-30,1	28,8-30,1	28,5-29,2	26,6-27,4	26,1-28,7	0-1,6	-	-	-	-	-	-	-	-	-	-	-	-	-
Philoscia muscorum	29,6-30,1	27,4-27,4	29,2-29,2	29,6-29,7	28,3-28,3	27,4-27,4	24,6-26,1	25,2-25,5	0-0	-	-	-	-	-	-	-	-	-	-	-	-
Philoscia affinis	27,8-29	26,8-27,5	27,4-29,1	27,7-30,3	27-28,5	26,3-27,2	22,5-24,6	23,4-24,1	16,8-17,9	0-3,1	-	-	-	-	-	-	-	-	-	-	-
Haplophtalmus danicus	30,5-31,5	29,5-30	29,5-30,2	30,6-32,1	25,7-26,4	24,1-24,9	27,5-31,3	26,8-27,4	24,6-25,1	23,6-25,7	0-1,7	-	-	-	-	-	-	-	-	-	-
Trichoniscus sp.	28,2-28,6	27,4-27,4	28,8-28,8	29-29,4	28,6-28,7	26,8-26,8	25-26,8	24,6-25	26,1-26,1	23,8-24,5	24,6-25,1	0-0	-	-	-	-	-	-	-	-	-
Trichoniscidae A	31,5-31,9	29-29	29,2-29,2	30,2-30,7	24,5-24,8	27,7-27,7	27,3-28,8	24,6-25	23-23	24,5-25	23,5-24,5	21,9-21,9	0-0	-	-	-	-	-	-	-	-
Hyloniscus riparius	29,7-30,6	27,4-27,9	28,9-29,5	28,7-30	23,5-24,3	23,7-24,2	23,5-26,2	21,9-22,5	22,6-23,7	22,5-24,9	21,9-22,6	22,4-23,2	22,5-23,1	0-1,4	-	-	-	-	-	-	-
Trichoniscidae B	28,6-28,9	26,6-26,6	28,6-28,6	30,2-30,9	26,2-26,3	24,5-24,5	25,5-26,6	24,7-24,7	22,3-22,3	21,1-22	22,8-23,5	22,3-22,3	26,6-26,6	20,7-21,4	0-0	-	-	-	-	-	-
Trichoniscus pusillus A	27,9-28,3	25,9-25,9	28,8-28,8	27,7-28	26,1-26,1	24,8-24,8	22,4-23,1	23-23,2	24,6-24,6	23,2-24,3	22,8-24,2	18,8-18,8	20,5-20,5	20,7-21,2	21,6-21,6	0-0	-	-	-	-	-
Trichoniscus pusillus B	28,4-29,1	27,2-27,5	28,9-29	28,7-29,2	28,1-28,5	24,9-25	21,4-22,9	22,5-23,2	23,6-23,7	22,5-23,7	22-22,8	19,1-19,2	21,1-21,2	20,2-21,1	21,1-21,8	11,4-11,7	0-0	-	-	-	-
Porcellionides pruinosus	29,8-30,3	27,5-28	30,1-30,3	30,6-31,5	25,4-25,7	25,2-25,7	24,4-26,3	26,4-26,8	22,4-22,6	21,5-23	24,9-25,9	22,2-22,5	23,2-23,4	20,3-22,4	23-23,4	23,4-23,8	24,5-25,1	0-0	-	-	-
Porcellio spinicornis	27,1-29,6	25,5-27,8	27,5-28,7	27,7-30,7	27,2-30,3	23,3-25,2	23-26	22,6-26,5	21,2-22	21,8-25,1	20,2-23,6	22,3-27,8	22,6-22,9	20,4-22,6	22,5-23,1	21,6-25,6	21-25,4	16,7-19,4	0-1,8	-	-
Armadillidium pictum	28-28,6	27,8-27,8	26,9-26,9	25,2-25,9	29,1-29,7	24,8-24,8	25,2-26,1	26,5-26,5	21,8-21,8	23,1-25,3	23,9-25,5	24,4-24,4	24,8-24,8	17,2-17,9	21,9-21,9	21,8-21,8	20,1-20,5	23,5-24,5	22,1-22,6	0-0	-
Armadillidium vesicolor A	26,5-27,4	23,6-24,3	25,9-25,9	25,5-26,1	27,4-27,8	23,7-23,7	23-24,8	23,2-23,2	22,6-22,6	21-21,8	22,5-23,2	21,2-21,7	25,5-25,5	22-22,6	20,5-20,5	22,5-22,5	21-21,3	22,4-22,8	18,3-19,8	19,2-19,7	0,9-0,9
Armadillidium vesicolor B	25,8-26,3	24,3-24,3	25,5-25,5	24,8-25,5	27,7-28	23,6-23,6	22,8-25,1	23,2-23,2	22,6-22,6	22,5-23,2	23,7-24,3	22,6-22,6	25,2-25,2	21,6-22,4	21,2-21,2	22,6-22,6	21,5-21,6	21,7-22	17,6-20,3	19,2-19,2	5,1-5,4
Armadillidium vesicolor C	26-26,4	23,7-23,7	26,3-26,3	26,1-26,7	27,4-27,6	23,4-23,4	22,8-24,8	21,9-22,3	21,4-21,4	20,9-21,9	23-23,6	21,7-21,7	24,5-24,5	22,4-22,9	20,7-20,7	22,1-22,1	21,4-21,7	20,5-20,7	16,8-18,5	19,2-19,2	4-4,3
Porcellio scaber A	28-28,6	24-24,1	27,2-27,9	27-27,9	25,5-26,3	22,6-22,8	23,6-25,7	24-24,8	22,8-23,2	21,1-22,1	21,9-22,7	24,5-24,8	25,4-26,1	21,9-22,5	21,2-21,3	23,2-23,4	22,1-22,5	21,1-21,4	18,3-20,5	17,5-17,9	14,7-15,1
Porcellio scaber B	27,2-30,2	24,8-25,5	26,1-29	25,6-28,3	26,1-27,9	22,2-24,3	23,4-26,9	22,8-26,5	22,1-23,5	21,4-26,1	19,2-23,8	24,1-26,1	23,5-27,1	18,8-23,2	18-21	21,4-23,3	23-24,1	20,5-22	16,7-18,8	16,1-17,3	13,4-15
Armadillidium vulgare A	28,4-29,4	25,7-26,3	27,5-28,5	27,4-29,2	27,2-27,6	23,8-24,7	24-26,4	22,8-23,3	22,8-23,5	21,9-23,2	21,4-22,5	20,8-21,3	23,7-24,3	21,9-23,3	21,5-21,8	20,4-21,3	20-21,5	19,9-20,5	19,9-24,3	18,6-21,3	13,8-14,4
Armadillidium vulgare B	27,5-28,3	24,6-25,1	26,8-27,2	26,7-27,5	26,5-27,4	24,5-25	23,9-25,5	21,1-22,3	23-23,2	21,3-22,6	22,4-23,8	21,7-22,4	24,8-25	21,6-22,6	21,4-21,8	19,8-20,1	19,7-20,2	20,8-21,6	19,3-23,3	17,2-19,2	13,8-14,1
Armadillidium vulgare C	26,9-28,3	24,8-25,8	26,4-27	26,4-27,6	26,1-27,8	24-24,5	24,3-26,2	22-22,7	21,7-22,8	20,3-22,5	21,6-22,4	21,2-22,3	23-24,1	21,8-22,6	21,2-21,5	20,3-21,3	20,1-20,8	19,7-20,5	19,2-22,9	18,9-19,7	13,9-14,5
Armadillidium vulgare E	27,5-27,9	25,9-26	27-27,3	27-27,8	27-27,8	23,9-24,9	24,8-26,1	21,4-22,5	22,3-22,8	21,2-22,5	22,2-23,1	21,7-23,1	23,6-23,7	22,3-23,1	21,4-21,8	19,9-20,5	19,9-20,4	20,3-20,8	18,5-22	18,4-18,4	13,8-15
Armadillidium vulgare D	27,5-28,3	24,3-25	26,6-26,8	26,4-27,6	25,8-27,2	24,2-25,2	23,1-26	21,2-22,6	21,9-23	19,2-22,1	21,9-22,6	20,3-21,2	22,3-23,7	21,6-22,7	20,1-21,1	19,2-19,9	18,8-20,1	19,5-20,8	18,8-22	13,3-18,4	13,6-14,3
Armadillidium sp.	26,5-27,5	24,3-24,8	25,4-25,5	25,4-26,1	24,6-25,2	23,6-23,9	22,7-24,6	21,4-21,7	21,7-21,9	19,7-21	21,9-22,8	20,8-21	23,7-24,3	19,6-21,4	20,9-21,6	21,4-21,7	21,3-21,7	18,1-18,3	18,7-20,6	17,5-17,9	13-14,1
Armadillidium opacum	27,6-28,1	24,8-24,8	27-27	27,7-28,4	26,2-26,5	23,7-23,7	23,9-25	23,7-23,9	23,1-23,1	22,4-23,1	24,2-25,4	23,1-23,1	24,8-24,8	20,2-20,6	21,5-21,5	22,9-22,9	22,8-23	19,8-20,2	19,1-20,6	22,6-22,6	16-16
Armadillidium camiolense	28,7-29,4	26,6-26,6	28-28	27,5-29	28,4-29,1	22-22	23,4-24,8	26,6-26,6	24,8-24,8	25,7-26,8	21,1-21,9	22,9-22,9	23,9-23,9	20,7-21,6	20,3-20,3	21,1-21,1	21,6-22,1	19,7-20,1	19,3-19,7	18,4-18,4	13,3-13,3
Lepidoniscus minutus	28,4-29,6	26,1-29	27,5-28,2	28,4-29,5	26,3-29,4	24,7-25,7	22-23,8	25,2-27,6	20,3-20,8	21,2-23,8	22-24	24,1-25,2	21,5-23,5	20,1-23,7	20,8-21,6	21-22,3	21,5-23,3	20,5-21,6	19,6-21,1	22,1-23,8	20,5-21,2
Porcellio laevis	30,2-30,8	24,8-24,8	29,5-29,5	28,4-30,1	29,1-29,3	21,4-21,4	24,7-26,5	24,8-25,6	23,9-23,9	26,2-27,4	24,4-25,5	24,8-24,8	23,9-23,9	19,3-20,5	17,1-17,1	22,6-22,6	21,9-22,2	20,5-21,4	20,5-21,4	22,7-22,7	23,5-23,5
Cylisticus convexus A	29,4-30	27,4-27,5	26,4-26,7	27,1-27,5	25,2-25,4	23,8-23,9	24,8-26,7	24,3-24,7	23-23,2	22,6-24,1	22,7-23,2	21,2-21,5	21,4-21,6	20,1-20,8	23,2-23,3	21,2-21,5	18,7-19	21,6-22	18,5-21,4	20,9-21,8	19-19,7
Cylisticus convexus B	29,3-30,3	26,4-27,7	27,2-28,6	27,9-29,6	24,8-25,4	22,8-23,6	23,9-26,8	24-25	23,2-24,1	22,8-25,6	21,8-23	22,1-22,3	21,7-22,4	20,7-22,3	21,8-22,2	21,7-22,3	19,4-19,8	21,3-22,2	20,3-21,9	21,4-22,1	17,6-18,6
Protracheoniscus franzi	27,6-28,2	27,3-27,3	26-26	26-27,5	31,3-32,3	23,3-23,3	24,2-25,4	28,2-28,2	25,6-25,6	27,8-29,3	21,6-23,7	24,7-24,7	19,8-19,8	18,6-19,4	19,9-19,9	22-22	22,9-23,3	20,3-21	20,7-21,1	18,6-18,6	17,2-17,6
Trachelipus rathkii A	28,4-28,8	26,8-26,8	29,2-29,2	29,7-30,3	25,7-25,7	23,4-23,4	22,8-24,4	25,7-25,9	20,8-20,8	20,7-21,4	22,7-23,2	23-23	21,4-21,4	22,3-23,2	23,3-23,3	21,6-21,6	21,1-21,6	20,3-20,5	18,3-22,4	24,4-24,4	20,8-20,8
Trachelipus rathkii B	27,2-28,6	26,5-28,2	28,7-29,5	27,1-30,5	24,8-27	23,8-25,6	22,3-24,4	24,9-26,4	20,9-22,5	19,7-23,3	22-23	21,8-23,3	19,4-21,9	17,1-23,7	22,2-23,4	21,2-22,5	19,8-21,7	19,3-21,2	18,3-23,3	21,7-23,8	20,1-22,9
Trachelipus rathkii C	26,8-28,3	27-29,3	28,5-30,2	28,8-30,1	25,6-26,1	23,9-25	21,5-24,8	25-26,3	20,3-22	19,7-23,9	21,6-24,7	21,6-24,9	18,5-21,9	16,6-22,8	22,7-25,4	21,9-22,9	20,2-22,3	19,1-21,3	17,3-21,5	20,6-23,1	18,9-21,5
Protracheoniscus sp.	28-28,4	25,4-25,4	25,4-25,4	26,3-27	26,3-26,5	22,8-22,8	22,3-24,8	25,9-26,1	23,4-23,4	21,6-23	21,3-21,9	22,8-22,8	22,8-22,8	22,7-23,3	21,4-21,4	21,6-21,6	20,8-21	20,9-21,4	18,3-19,8	20,5-20,5	18,5-18,7
Protracheoniscus politus	26,9-28,1	23,8-25,4	25-27,5	24,2-28,2	25,5-26,8	22-23,4	20,6-22,9	23,6-26,3	23,5-24,2	21,9-27,1	21,3-24,3	21,2-22,2	20,3-24,5	18,3-22,6	21,4-21,8	18,6-22,6	17,8-21,7	19,7-20,7	19,2-23,2	19,2-21,1	17,9-19,2
Porcellium collicola A	29,6-30,1	26,5-26,8	28,7-29,1	29,2-30	24,1-24,5	23,2-23,4	24,3-25	25,4-26,1	21,1-21,2	21,9-23,4	21,7-22,3	20,5-20,7	20,5-20,7	22-22,7	22-22	21,2-21,4	20,7-20,9	19,9-20,5	18,6-19,8	21,4-21,9	18-18,3
Porcellium collicola B	27,5-29,2	25,2-26	27,8-28,5	27,6-28,9	25-25,7	23,3-23,9	22,3-25,8	25,4-26,5	23,1-23,6	22,5-24	24,4-25,9	22,4-23,3	23,3-23,9	20-22,3	21-21,5	21,8-22,7	20,6-21,5	21,7-22,7	17,6-20,8	22,4-23,8	17,4-18,4
Porcellium conspersum	25,7-26,8	26,4-28,1	26,3-27,7	26,3-28,6	25,9-30,5	22,2-24,8	23,2-26,7	25,5-30,5	24,1-26,9	22,8-28,7	23,2-26,9	22,6-26,3	21-23,7	23,4-25,2	25,1-25,2	21,7-23,4	19,8-20,4	22-23,2	17,4-20,6	22,3-23,5	17,8-19,8
Armadillidium nasatum	29,8-30,4	27,5-27,5	27,1-27,1	26,3-27,5	28,8-29,4	22,1-22,1	24,6-25,8	28,3-28,3	25,8-25,8	27,1-28,9	23,8-25,2	23,8-23,8	20,8-20,8	20,8-22,3	25,2-25,2	20,8-20,8	19,6-19,6	20,8-22,3	20-21,1	23,9-23,9	22,9-23,3
Trachelipus nodulosus	29,7-30,3	25,8-25,8	27,6-27,6	28,8-29,1	25,8-25,8	23,1-23,1	23,9-24,4	27,6-28,1	24-24	24,9-25,3	19,5-21,1	25,3-25,3	18,1-18,1	21,3-22,2	19,5-19,5	18,1-18,1	17,6-18	21,3-22,5	19,5-20,4	23,2-23,2	21,3-21,3
Trachelipus ratzeburgii A	28,1-30,8	25,5-26,3	26,5-27,7	26,3-28,2	24,9-26,1	21,5-22,9	23,9-27,4	22,6-23,6	23-23,7	23,8-25,1	22,9-25,8	19,4-21,2	23,3-24,4	20,6-22,1	21,2-22,2	18,8-20,9	16,4-18,5	20,9-21,9	18,3-24,2	17,5-18,9	18-18,7
Trachelipus ratzeburgii B	29-29,3	26,1-26,1	29-29	29,2-29,7	25,5-25,6	24,3-24,3	23,1-26,8	23,9-24,3	24,1-24,1	25,6-26,1	24,5-25,7	21-21	24,1-24,1	23-23,7	23,1-23,1	20,5-20,5	20,7-20,8	22,1-22,4	21,6-24,7	19,7-19,7	19,4-19,4
Trachelipus ratzeburgii C	27,6-29	25,2-26,2	27-28,4	27,5-28,6	24,7-25,7	23,2-24,3	20,4-25,1	21,6-23,6	21,6-23,4	22,1-25,1	23,2-25,4	19,7-21,4	21,7-21,9	21,6-23,3	20,5-21,6	19,6-20,8	18,5-19,2	18,2-21,8	16,3-24,7	15,1-18,4	17,6-19,1

vesicolor B	Armadillidium vesicolor C	Porcellio scaber A	Porcellio scaber B	Armadillidium vulgare A	Armadillidium vulgare B	Armadillidium vulgare C	Armadillidium vulgare E	Armadillidium vulgare D	Armadillidium sp.	Armadillidium opacum	Armadillidium carniolense	Lepidoniscus minutus	Porcello laevis	Cylisticus convexus A	Cylisticus convexus B	Protracheoniscus franzi	Trachelipus rathkii A	Trachelipus rathkii B	Trachelipus rathkii C	Protracheoniscus sp.	Protracheoniscus politus	Porcellium collicola A	Porcellium collicola B	Porcellium conspersum	Armadillidium nasatum	Trachelipus nodulosus	Trachelipus ra
-	-	-	-	-	-	-	-	-	-	-	-	-	-	-	-	-	-	-	-	-	-	-	-	-	-	-	
-	-	-	-	-	-	-	-	-	-	-	-	-	-	-	-	-	-	-	-	-	-	-	-	-	-	-	
-	-	-	-	-	-	-	-	-	-	-	-	-	-	-	-	-	-	-	-	-	-	-	-	-	-	-	
-	-	-	-	-	-	-	-	-	-	-	-	-	-	-	-	-	-	-	-	-	-	-	-	-	-	-	
-	-	-	-	-	-	-	-	-	-	-	-	-	-	-	-	-	-	-	-	-	-	-	-	-	-	-	
-	-	-	-	-	-	-	-	-	-	-	-	-	-	-	-	-	-	-	-	-	-	-	-	-	-	-	
-	-	-	-	-	-	-	-	-	-	-	-	-	-	-	-	-	-	-	-	-	-	-	-	-	-	-	
-	-	-	-	-	-	-	-	-	-	-	-	-	-	-	-	-	-	-	-	-	-	-	-	-	-	-	
-	-	-	-	-	-	-	-	-	-	-	-	-	-	-	-	-	-	-	-	-	-	-	-	-	-	-	
-	-	-	-	-	-	-	-	-	-	-	-	-	-	-	-	-	-	-	-	-	-	-	-	-	-	-	
-	-	-	-	-	-	-	-	-	-	-	-	-	-	-	-	-	-	-	-	-	-	-	-	-	-	-	
-	-	-	-	-	-	-	-	-	-	-	-	-	-	-	-	-	-	-	-	-	-	-	-	-	-	-	
-	-	-	-	-	-	-	-	-	-	-	-	-	-	-	-	-	-	-	-	-	-	-	-	-	-	-	
-	-	-	-	-	-	-	-	-	-	-	-	-	-	-	-	-	-	-	-	-	-	-	-	-	-	-	
-	-	-	-	-	-	-	-	-	-	-	-	-	-	-	-	-	-	-	-	-	-	-	-	-	-	-	
-	-	-	-	-	-	-	-	-	-	-	-	-	-	-	-	-	-	-	-	-	-	-	-	-	-	-	
-	-	-	-	-	-	-	-	-	-	-	-	-	-	-	-	-	-	-	-	-	-	-	-	-	-	-	
-	-	-	-	-	-	-	-	-	-	-	-	-	-	-	-	-	-	-	-	-	-	-	-	-	-	-	
-	-	-	-	-	-	-	-	-	-	-	-	-	-	-	-	-	-	-	-	-	-	-	-	-	-	-	
-	-	-	-	-	-	-	-	-	-	-	-	-	-	-	-	-	-	-	-	-	-	-	-	-	-	-	
-	-	-	-	-	-	-	-	-	-	-	-	-	-	-	-	-	-	-	-	-	-	-	-	-	-	-	
-	-	-	-	-	-	-	-	-	-	-	-	-	-	-	-	-	-	-	-	-	-	-	-	-	-	-	
0-0	-	-	-	-	-	-	-	-	-	-	-	-	-	-	-	-	-	-	-	-	-	-	-	-	-	-	
3,4-3,4	0-0	-	-	-	-	-	-	-	-	-	-	-	-	-	-	-	-	-	-	-	-	-	-	-	-	-	
15,5-15,6	14,9-15,1	0-0	-	-	-	-	-	-	-	-	-	-	-	-	-	-	-	-	-	-	-	-	-	-	-	-	
13,8-15,6	12,6-13,9	4,3-5,8	0-2,5	-	-	-	-	-	-	-	-	-	-	-	-	-	-	-	-	-	-	-	-	-	-	-	
14-14,8	13,2-13,9	16,2-16,8	14,9-16,8	0-0,4	-	-	-	-	-	-	-	-	-	-	-	-	-	-	-	-	-	-	-	-	-	-	
14-14,3	13,1-13,4	16,1-17	13,4-16,5	3,4-3,8	0-2,2	-	-	-	-	-	-	-	-	-	-	-	-	-	-	-	-	-	-	-	-	-	
14,4-14,9	13-13,4	15,1-16,8	12,9-16,6	4,7-6,5	4,7-6,2	0-3,6	-	-	-	-	-	-	-	-	-	-	-	-	-	-	-	-	-	-	-	-	
14,3-15	12,9-13,9	15,7-16,3	13,7-15,8	3,8-4,7	3,4-4	2,5-4,5	0-2	-	-	-	-	-	-	-	-	-	-	-	-	-	-	-	-	-	-	-	
13,9-14,7	12,6-13,2	15,3-16,5	10,4-16,1	4,4-5,7	4-5,3	2,5-4,9	2,2-4,2	0-2,4	-	-	-	-	-	-	-	-	-	-	-	-	-	-	-	-	-	-	
13,9-14,9	12,9-13,8	17,6-18,3	13,2-17	11,1-11,9	11,2-12,1	11,8-13	10,9-11,4	11,5-11,9	1,8-1,8	-	-	-	-	-	-	-	-	-	-	-	-	-	-	-	-	-	
16,9-16,9	14,7-14,7	17,6-17,8	15,8-18,1	13,8-14,2	13,8-14,3	13,8-14,1	14,3-15	13,7-14,5	13-13	0-0	-	-	-	-	-	-	-	-	-	-	-	-	-	-	-	-	
15,6-15,6	13,3-13,3	16,8-17	14,2-16,3	12,6-15,1	11,1-12,8	11,5-13	11,8-11,9	10,6-11,8	9,2-10,1	9,2-9,2	0-0	-	-	-	-	-	-	-	-	-	-	-	-	-	-	-	
21-24,3	20,5-22	18,8-19,8	15,1-20,8	18,4-22	17,9-20,1	17,4-20,2	17,6-20,1	16,1-19,2	19,7-21,5	17,3-20,5	17,4-17,9	0-1,4	-	-	-	-	-	-	-	-	-	-	-	-	-	-	
24,4-24,4	23,1-23,1	17,9-19,7	17,6-19,2	20,9-22,3	19,2-19,7	19,7-23,1	19,2-19,7	17-18,7	18,8-20,9	21,8-21,8	18,8-18,8	15,1-18,7	0-0	-	-	-	-	-	-	-	-	-	-	-	-	-	
19-19,2	19-19,3	20,5-21	18,8-21,7	19,1-20	18,7-19,3	18,5-19	19,1-19,5	18,3-19,2	18,1-18,2	18,5-18,8	15,6-16,3	18,8-21,7	18,7-19,2	0-0	-	-	-	-	-	-	-	-	-	-	-	-	
19-19,9	18,8-19,4	19-20	19,2-20,6	18,8-20	18,8-19,7	17,8-18,5	18,3-19,2	17-18,3	17,6-18,3	18,7-19,7	15,1-16,6	19,2-21,6	19,5-20,9	6,1-6,3	0-2,4	-	-	-	-	-	-	-	-	-	-	-	
19,4-19,4	18,5-18,5	15,3-15,9	15,9-17,1	16,1-16,9	17,3-17,6	16,8-18,8	16,3-16,7	16,1-16,9	17,2-18,9	20,3-20,3	18,1-18,1	19,8-19,8	21,6-21,6	18,5-19,2	17,6-19,1	0-0	-	-	-	-	-	-	-	-	-	-	
20,7-20,7	20,5-20,5	18,4-19	18,6-21,8	19,1-19,8	18,7-19,2	18,5-19	18,5-18,7	16,8-18,1	19,9-19,9	20,6-20,6	18,8-18,8	19,4-21	16,7-16,7	18,8-19,2	17,5-18,8	23,8-23,8	0-0	-	-	-	-	-	-	-	-	-	
20,1-23,8	19,6-22,9	17,8-20,3	18,4-22	18,5-23,8	18,1-21,1	17,6-21,6	17,8-20,7	14,8-19,4	18,1-20,3	20,2-20,9	18-19,3	19,2-22	16,7-18,8	16,1-19,2	14,2-18,5	22,5-25	2,9-4	0-2,4	-	-	-	-	-	-	-	-	
19,5-22	18,8-20,5	17,4-20	17,2-21,8	18,9-22,9	18,5-21	18,1-21,4	17,9-20,5	13,3-19	18,5-19,4	19,6-20,2	18,1-19,3	18,7-20,6	17,1-17,7	16,1-19,2	14,6-18,5	23,6-24,2	3,5-5,4	1,8-5,1	0-3,9	-	-	-	-	-	-	-	
17,6-17,6	16,8-16,8	18,5-18,6	18,4-19,4	18,2-18,8	19,1-19,6	18,9-19,2	19,2-19,4	18,1-19,4	17,8-17,8	18,9-18,9	18,3-18,3	20,3-21	21,8-21,8	17,6-17,7	17,8-18,7	15,9-15,9	20,8-20,8	19,5-22	20-23,9	0-0	-	-	-	-	-	-	
18,2-19,1	17-17,9	19,4-20,7	19,3-22,4	16,4-20,5	16-19,1	16,4-18,7	16,9-17,8	16,1-17,4	16,1-17,5	18,5-19,1	16,1-17,2	19,5-21,7	20,4-21,5	15,7-18,8	15,7-19	14,5-15,7	18,2-19,5	16,8-19,2	17,1-19,9	13,9-14,7	0-1,3	-	-	-	-	-	
17,6-17,9	17,2-17,6	17,8-18	15,8-18,5	16,2-17	16,7-17,8	16,2-17,6	17,1-17,6	16,9-17,4	17,8-18,3	17,8-18	15,2-16	17,8-19	21,5-21,8	15,8-16,2	15,8-17,2	15,9-16,3	18,7-19	18,5-21,6	18,6-21,5	15,9-16,2	14-16,2	0-0,2	-	-	-	-	
17,9-18,7	16,7-17,5	19,4-20,6	18,4-20,4	19,6-20,5	19-20,3	18,5-19,8	19,2-20,3	18,2-19,4	19,4-20,2	19,3-19,7	17,1-18,2	19,2-23,7	19,6-20,5	17,6-18,5	16,9-19,1	16,1-17,8	18,8-19,5	19,6-22,2	17,8-22,1	16,1-17,2	13,6-16,1	13-13,9	0-0	-	-	-	
17,4-17,8	16,2-17,2	20,3-21	20,8-22,7	19,1-22,4	18,5-22,8	19,1-24	19,4-22,8	18,3-21,2	19,2-22,2	20,9-22,2	20,6-21	21-24,3	21,6-24,4	16,2-19,5	16,2-19,1	16,2-19,8	20,3-21,6	19,6-22,9	18,8-22,8	15,6-15,8	13,8-15,3	12,6-15,1	10,9-14,4	0-1,2	-	-	
22,9-22,9	22,1-22,1	21,7-21,7	20,9-21,8	19,4-21,1	19,7-20,4	20,1-21,7	18,8-19,6	20,3-22	21,7-21,7	22,5-22,5	19,3-19,3	20,2-21,7	22,2-22,2	15-15,3	15,4-16,3	18,5-18,5	22,5-22,5	21,7-23,6	22,1-22,9	20,8-20,8	17,6-18,8	14,2-14,5	15,1-15,4	13,2-15	0-0	-	
22,6-22,6	20,8-20,8	22,2-23,9	21,7-24	21,3-23,4	20,8-21,7	21,3-21,9	21,7-21,9	19,7-21,7	23,1-23,5	19,5-19,5	20,6-20,6	23,8-24	19-19	20-20,8	18,1-20,4	24,7-24,7	16,7-16,7	16,7-17,3	17,6-18,5	22,6-22,6	21,2-22,4	19,5-19,5	17,4-20,2	22,2-23,1	21,7-21,7	0-0	
17,3-18,3	17,2-18	18,2-19,4	17,6-19,7	19,5-20,6	19,6-21,2	20,2-21,9	20-21	18,2-20,2	18,7-20,5	20-21	18,3-20,1	20,5-23	19,7-21,4	18,4-19,5	17,5-19,2	22,5-23,2	17,3-18,1	16,6-18,6	16,3-19	18,1-19,2	17,4-20,1	17,2-18,5	19-20,1	19,6-22,2	19,2-20	16,7-17,4	
19,4-19,4	18,7-18,7	20,7-20,7	19,2-19,9	20,6-21,5	19,8-20,8	20,1-21,8	20,7-21,2	20,1-20,7	19-19,7	21,8-21,8	18,8-18,8	19,2-22,2	20,5-20,5	19,2-19,5	18,9-19,3	21,1-21,1	18,3-18,3	17,7-19,4	17,5-19	19-19	16,1-20,1	18,9-19	20,4-21,1	21-22,2	20,4-20,4	19-19	
16,1-17,9	15,5-16,7	17,4-18,6	14-17,8	17,1-19,8	17,9-20,4	17,6-19,7	17,4-19,6	17,1-19	16,1-18,7	18,2-20,6	15,6-18,8	15,1-21,4	15,1-20,9	19,2-20,5	18,2-19,6	15,9-20,7	17,1-18,9	14-18,9	14,1-19,1	15,8-18,3	13,7-20,2	17,4-18,7	19,2-20,7	15,9-22,8	14,1-20	12,5-16,7	

atzeburgii A	Trachelipus ratzeburgii B	Trachelipus ratzeburgii C
-	-	-
-	-	-
-	-	-
-	-	-
-	-	-
-	-	-
-	-	-
-	-	-
-	-	-
-	-	-
-	-	-
-	-	-
-	-	-
-	-	-
-	-	-
-	-	-
-	-	-
-	-	-
-	-	-
-	-	-
-	-	-
-	-	-
-	-	-
-	-	-
-	-	-
-	-	-
-	-	-
-	-	-
-	-	-
-	-	-
-	-	-
-	-	-
-	-	-
-	-	-
-	-	-
-	-	-
-	-	-
-	-	-
-	-	-
-	-	-
-	-	-
-	-	-
-	-	-
-	-	-
-	-	-
-	-	-
-	-	-
-	-	-
0-1,1	-	-
9,1-10,4	0-0	-
6,3-9,5	5-6,6	0-3,2